

1

2 Alterations in cortical excitability during pain: A combined TMS-EEG Study

3 Nahian S Chowdhury^{1,2}, Alan KI Chiang^{1,2}, Samantha K Millard^{1,2}, Patrick Skippen¹, Wei-Ju

4 Chang^{1,3}, David A Seminowicz^{1,6}, Siobhan M Schabrun^{1,7}

5 **Affiliations**

6 ¹Center for Pain IMPACT, Neuroscience Research Australia, Sydney, New South Wales,

7 Australia, ²University of New South Wales, Sydney, New South Wales, Australia, ³School of

8 Health Sciences, College of Health, Medicine and Wellbeing, The University of Newcastle,

9 Callaghan, New South Wales, Australia, ⁶Department of Medical Biophysics, Schulich School

10 of Medicine & Dentistry, University of Western Ontario, London, Canada, ⁷The Gray Centre

11 for Mobility and Activity, University of Western Ontario, London, Canada.

12 **Corresponding author**

13 Nahian S Chowdhury

14 Email: n.chowdhury@neura.edu.au

15 Neuroscience Research Australia, 139 Barker Street Randwick 2031 NSW

16 **Disclosures**

17 The authors have no conflicts of interest to declare.

18

19

20

21

22

23

24

25

26

Abstract

27 Transcranial magnetic stimulation (TMS) has been used to examine inhibitory and
28 facilitatory circuits during experimental pain and in chronic pain populations. However,
29 current applications of TMS to pain have been restricted to measurements of motor evoked
30 potentials (MEPs) from peripheral muscles. Here, TMS was combined with
31 electroencephalography (EEG) to determine whether experimental pain could induce
32 alterations in cortical inhibitory/facilitatory activity observed in TMS-evoked potentials
33 (TEPs). In Experiment 1 ($n = 29$), multiple sustained thermal stimuli were administered to the
34 forearm, with the first, second and third block of thermal stimuli consisting of warm but non-
35 painful (pre-pain block), painful (pain block) and warm but non-painful (post-pain block)
36 temperatures respectively. During each stimulus, TMS pulses were delivered while EEG (64
37 channels) was simultaneously recorded. Verbal pain ratings were collected between TMS
38 pulses. Relative to pre-pain warm stimuli, painful stimuli led to an increase in the amplitude
39 of the frontocentral negative peak \sim 45ms post-TMS (N45), with a larger increase associated
40 with higher pain ratings. Experiments 2 and 3 ($n = 10$ in each) showed that the increase in the
41 N45 in response to pain was not due to changes in sensory potentials associated with TMS, or
42 a result of stronger reafferent muscle feedback during pain. This is the first study to use
43 combined TMS-EEG to examine alterations in cortical excitability in response to pain. These
44 results suggest that the N45 TEP peak, which indexes GABAergic neurotransmission, is
45 implicated in pain perception and is a potential marker of individual differences in pain
46 sensitivity.

47

48

49

50

51

52

53

54

Introduction

55 Pain is a complex subjective experience, and understanding how pain is processed
56 remains a challenge (Apkarian, 2021). Several neuroimaging techniques have been applied
57 to disentangle these complexities: functional magnetic resonance imaging has assisted in
58 identifying brain structures implicated in pain processing (Reddan & Wager, 2018), while
59 electroencephalography (EEG) has contributed to our understanding of the temporal sequence
60 of pain processing (Ploner & May, 2018). Another useful technique that has been used to
61 examine the role of inhibitory and facilitatory neural circuits in pain has been transcranial
62 magnetic stimulation (TMS) delivered to the brain (Chang et al., 2018; Schabrun & Hodges,
63 2012). However, current applications of TMS to pain have involved recording the output of
64 TMS from a muscle, a signal that could be influenced by many intermediate (subcortical,
65 spinal, peripheral) factors, and which restricts investigations to the motor system only. Here,
66 we use a combined TMS-EEG measure to record output of TMS directly from the cortex and
67 from multiple brain regions, in pain-free and tonic pain conditions.

68 When TMS is delivered over the primary motor cortex (M1), a magnetic pulse
69 induces an electrical current in underlying cortical tissue that, if the intensity is sufficient,
70 activates corticomotor pathways, inducing a motor evoked potential (MEP) in a target
71 muscle. The magnitude of the MEP serves as an index of corticomotor excitability. Past
72 systematic reviews on studies measuring MEPs during acute experimental pain (Bank, Peper,
73 Marinus, Beek, & Van Hilten, 2013; Burns, Chipchase, & Schabrun, 2016; Chowdhury et al.,
74 2022; Rohel et al., 2021) have shown a reduction in MEP amplitude during pain and after
75 pain resolution, with stronger reductions in MEP amplitude associated with lower acute pain
76 severity (Chowdhury, et al., 2022). It has been hypothesised that this reduction in MEP
77 amplitude is an adaptive mechanism that restricts movement in the pain-afflicted area, to
78 protect the area from further pain and injury (Hodges & Tucker, 2011).

79 While previous findings show promise for the use of TMS to discover and validate
80 potential biomarkers for pain, limitations exist when using TMS to measure MEPs. First,
81 MEP responses to TMS reflect the net sum of cortical, spinal, and peripheral activity within
82 the corticomotor pathway. This makes it unclear as to whether pain processes occur at the
83 cortical, spinal or peripheral level. Further, measurement of MEPs restricts investigations to
84 M1. One way of overcoming these limitations is by combining TMS and EEG to measure
85 TMS-evoked potentials (TEPs). TEPs index cortical excitability *directly* from the cortex (i.e.
86 without influence of subcortical, spinal and peripheral processes), as well as from regions
87 *outside M1* (Farzan et al., 2016). TEPs also provide an index of the activity of specific
88 neurotransmitter circuits within the cortex. For example, TEP peaks that occur at ~45ms and
89 100ms post-stimulation are linked to GABA_A and GABA_B neurotransmission respectively
90 (Premoli et al., 2014), while the TEP peak ~60ms post-stimulation is linked to glutamatergic
91 neurotransmission (Belardinelli et al., 2021). Overall, TEPs provides additional spatial and
92 temporal information about cortical activity over MEPs, making it ideal for understanding the
93 brain mechanisms involved in pain perception.

94 TEPs have already shown potential to serve as a biomarker for the development and
95 prognosis of various neurological and psychiatric conditions (for reviews see (Kallioniem &
96 Daskalakis, 2022; Tremblay et al., 2019)). However, the applicability of TEPs to pain
97 research is yet to be established. While GABAergic processes indexed by TEPs have been
98 hypothesised to be involved in pain (Barr, Farzan, Davis, Fitzgerald, & Daskalakis, 2013),
99 direct evidence is scarce. Two studies (Che et al., 2019; Ye, Wang, & Che, 2022) examined
100 whether the potential analgesic effects of repetitive TMS (rTMS) over the dorsal prefrontal
101 cortex are associated with plasticity in TEPs. These studies separately measured TEPs and
102 ratings to painful stimuli, before and after rTMS, with one finding that increases in pain
103 thresholds following rTMS were associated with changes in TEPs that index GABAergic

104 processes (Ye et al., 2022). While these studies assist us in understanding whether TEPs
105 might mediate rTMS-induced pain reductions, no study has investigated whether TEPs are
106 altered in direct response to pain.

107 The aim of the present study was to use TMS-EEG to determine whether acute
108 experimental pain induces alterations in cortical inhibitory and facilitatory peaks observed
109 using TEPs. We used a tonic heat pain paradigm (Furman et al., 2020; Granot, Granovsky,
110 Sprecher, Nir, & Yarnitsky, 2006), in which multiple thermal stimuli were applied over the
111 right extensor carpi radialis brevis (ECRB) muscle via a thermode. For each thermal
112 stimulus, the temperature increased from a neutral baseline of 32°C to either a warm non-
113 painful or a painful (46°C) temperature, with this temperature maintained for 40 seconds.
114 During this time, TMS was administered to the left M1 with concurrent EEG to obtain TEPs
115 from 63 scalp channels, and MEPs from the ECRB muscle (see Figure 1). Verbal pain ratings
116 were obtained between pulses. It was hypothesized that TEP peaks that index GABAergic
117 processes, including the peaks at ~45 and 100ms after TMS, would increase in response to
118 painful stimuli relative to warm non-painful stimuli.

119 **Results**

120 **Experiment 1 – Does acute pain alter cortical excitability?**

121 In Experiment 1 (n = 29), we determined whether painful thermal stimuli induced
122 alterations in TEP peaks relative to a non-painful baseline. The protocol (Figure 2) consisted
123 of three blocks of stimuli, in chronological order: pre-pain, pain, and post-pain blocks. The
124 pre-pain and post-pain blocks each consisted of six 40s thermal stimuli (20s interstimulus
125 interval) delivered at a non-painful temperature (calibrated to each participant's warmth
126 detection threshold), while the pain block consisted of six 40s thermal stimuli delivered at
127 46°C. The pre-pain/pain/post-pain design has been commonly used in the TMS-MEP pain
128 literature, as many studies have demonstrated strong changes in corticomotor excitability that

129 persist beyond the painful period. Indeed, in a systematic review, we showed effect sizes of
130 0.55-0.9 for MEP reductions 0-30 minutes after pain had resolved (Chowdhury et al., 2022).
131 As such, if we had used an alternative design with blocks of warm stimuli intermixed with
132 blocks of painful stimuli, the warm stimuli blocks would not serve as a valid non-painful
133 baseline. Based on a previous study (Dubé & Mercier, 2011) which also used sequences of
134 painful (50°C) and warm (36°C) thermal stimuli, we did not anticipate that the stimulus in the
135 pain block would entrain pain in the post-pain block.

136 Prior to the test blocks, we measured warmth, cool, and pain detection thresholds to
137 ascertain whether: a) participants could perceive increases or decreases in the thermode
138 temperature relative to a neutral baseline of 32°C, and b) the pain detection threshold was
139 below 46°C. All participants were able to detect increases or decreases in temperature from
140 baseline. The mean (\pm SD) cool and warmth detection threshold was $28.6 \pm 1.9^\circ\text{C}$ and $35.1 \pm$
141 1.5°C respectively. All participants reported a heat pain threshold that was above their
142 warmth detection threshold and below the test temperature of 46°C. The mean heat pain
143 threshold was $41.2 \pm 2.8^\circ\text{C}$.

144 All participants reported 0/10 pain during the pre-pain and post-pain blocks, and pain
145 ratings varying between 1-10 during the pain block. Figure 3 shows the mean pain ratings for
146 the ten pain measurements of each of the six painful stimuli delivered during the pain block
147 (~4 seconds in between pain measurements). A 6 (stimulus number: 1-6) \times 10 (timepoint:1-
148 10) Bayesian repeated measures ANOVA revealed anecdotal evidence (i.e., no conclusive
149 evidence) of a difference in pain between six thermal stimuli ($\text{BF}_{10} = 2.86$). However, there
150 was very strong evidence for a difference in pain ratings between the ten timepoints ($\text{BF}_{10} =$
151 6.1^{30}). There was also strong evidence of an interaction between stimulus number and
152 timepoint, suggesting the time course of pain across the 40 seconds thermal stimulus differed
153 across the six thermal stimuli of the pain block ($\text{BF}_{10} = 19.6$). Overall, although there was no

154 conclusive evidence for pain differing *between* successive stimuli, there was evidence that
155 pain fluctuated *during* each 40 second stimulus.

156 The mean resting motor threshold (RMT) and test intensity of TMS was (mean \pm SD)
157 $70.7 \pm 8.5\%$ and $77.7 \pm 9.2\%$ of maximum stimulus output respectively. We note that the
158 relatively high RMTs are likely due to aspects of the experimental setup that increased the
159 distance between the TMS coil and the scalp, including the layer of foam placed over the coil,
160 the EEG cap and relatively thick electrodes (6mm). Three participants were excluded from
161 the MEP analysis due to EMG software failure – these participants were still included in the
162 TEP analysis. A Bayesian repeated-measures ANOVA was run to compare MEP amplitudes
163 between pre-pain, pain and post-pain conditions. There was anecdotal evidence of a
164 difference in MEP amplitude between blocks ($BF_{10} = 1.02$) (Figure 4A). A Bayesian
165 correlation test was also run to determine whether the mean pain rating (across blocks and
166 timepoints) was associated with the change in MEP amplitude during pain as a proportion of
167 pre-pain. These MEP change values were log-transformed as they were not normally
168 distributed according to a Shapiro-Wilk Test ($W = .58, p < .001$). There was strong evidence
169 for a positive relationship ($r_{26} = 0.54, BF_{10} = 11.17$) (Figure 4B). such that participants who
170 showed a larger reduction in MEP amplitude during pain reported lower pain ratings.

171 One participant was excluded from the TEP analysis due to failure to save the
172 recording during the experiment, though this participant was still included in the MEP
173 analysis. One participant had missing post-pain data as the TMS coil had overheated during
174 this portion of the experiment – their data were still included for the pre-pain vs. pain
175 comparison. Figure 5 shows the grand average TEPs for all 63 channels, across pre-pain, pain
176 and post-pain conditions, as well as the scalp topographies at timepoints where TEP peaks are
177 typically observed – N15, P30, N45, P60, N100 and P180ms (Farzan et al., 2016). Source
178 reconstruction using a co-registered template brain model was also conducted to characterise

179 source activity at each timepoint (Figure 5). For the N15 and P30 peaks, there was higher
180 current density in the left motor areas, consistent with previous studies suggesting that TMS
181 evoked activity at 15 and 30ms after the TMS pulse reflect early excitation of motor areas
182 ipsilateral to the stimulated region (Farzan & Bortoletto, 2022). For the N45 and P60 peaks,
183 there was higher current density in the left motor and somatosensory areas at 45 and 60ms
184 after the TMS pulse, consistent with previous studies showing a sensorimotor origin a these
185 timepoints (Ahn & Fröhlich, 2021), however higher current density was also present in the
186 left parietal and right sensorimotor areas. For the N100 and P180 peaks, there was higher
187 current density in the central regions, mostly contralateral to the stimulated cortex. Overall,
188 we found consistencies in the source localization with previous studies, including a
189 sensorimotor origin of early peaks from 15-60ms. However, we did not directly compare
190 source activity between conditions due to the inaccuracies involved in source estimation in
191 the absence of co-registered magnetic resonance imaging (MRI) scans (Brodbeck et al., 2011;
192 Michel & Brunet, 2019) and EEG electrode location digitization (Shirazi & Huang, 2019).

193 Comparisons of TEP amplitude between conditions were based on the electrode-space
194 data. However, as this is the first study investigating the effects of experimental pain on TEPs
195 amplitude, there were no *a priori* regions or timepoints of interest to compare between
196 conditions. A statistically robust starting point in these situations is to use a cluster-based
197 permutation analysis (Frömer, Maier, & Abdel Rahman, 2018). This analysis was used to
198 compare amplitudes between pre-pain and pain, and pre-pain and post-pain, at each timepoint
199 and for each electrode. We found that during pain relative to pre-pain, there was a
200 significantly larger negative amplitude ($p = .021$) at frontocentral electrodes and a
201 significantly larger positive amplitude at parietal-occipital electrodes ($p = .028$), specifically
202 between 43-90ms after the TMS pulse. No significant differences in TEP amplitude were
203 found when comparing the pre-pain and post-pain conditions, and pain and post-pain

204 conditions. As such, the subsequent TEP peak analyses were focused on the pre-pain vs. pain
205 comparison, while the pre-pain vs. post-pain and pain vs. postpain comparisons are presented
206 in the supplementary material.

207 Figure 6A shows the grand average TEP waveform at the frontocentral electrodes
208 ('AF3','AFz','AF4','F1','Fz','F2','F4','FC2','FC4') identified from the cluster analysis for the
209 pre-pain vs. pain conditions (Supplementary Figure 1 shows the pre-pain vs. post-pain
210 comparison). Two peaks at ~45 and 85ms after the TMS pulse are visible in the time window
211 where the significant cluster was detected. Given the approximate timing, these peaks are
212 likely to be the N45 peak and an early N100 peak. The amplitude of these peaks was
213 identified for each participant using the TESA peak function (Rogasch et al., 2017) with
214 defined time windows of 40-70 and 75-95ms for the first and second peak respectively.

215 These time windows were chosen to account for variation between participants in the latency
216 of the first and second peak. Bayesian paired-sample t-tests showed very strong evidence that
217 the first peak at ~45ms ($BF_{10} = 57.21$) and moderate evidence that the second peak at ~85ms
218 ($BF_{10} = 6.77$) had larger amplitude during the pain block compared to the pre-pain block.

219 Figure 6B shows the individual level relationship between the mean pain rating, and the
220 difference in N45 and N100 amplitude between pain and pre-pain. There was strong evidence
221 that participants who reported higher pain ratings also showed a larger increase in N45 peak
222 amplitude during the pain block ($r_{26} = 0.52$, $BF_{10} = 10.64$). There was anecdotal evidence for
223 no association between pain ratings and changes in the N100 peak amplitude during pain (r_{26}
224 = 0.24, $BF_{10} = 0.48$).

225 Figure 6C shows the mean TEP waveform of the parietal-occipital electrodes
226 ('P1','PO3','O1','CPz','Pz','Pz','Oz','CP2','P2','PO4','O2','CP4','P4') identified from the cluster
227 analysis for the pre-pain vs. pain conditions (Supplementary Figure 1 shows the pre-pain vs.
228 post-pain comparison). One peak at ~50ms is visible in the time window where the

229 significant cluster was detected. The approximate timing of this peak is consistent with the
230 commonly identified P60. The amplitude of this peak was identified for each participant with
231 a defined time window of 35 to 65ms. This time window was chosen to account for variation
232 between participants in the latency of the peak. There was moderate evidence that the peak at
233 ~50ms was stronger during the pain block compared to pre-pain block ($BF_{10} = 5.56$). Figure
234 6D shows the individual level relationship between the mean pain rating and the difference in
235 the P60 amplitude between pain and pre-pain. There was anecdotal evidence in favour of no
236 relationship between pain ratings and changes in P60 amplitude during the pain block ($r_{26} =$
237 0.21, $BF_{10} = 0.407$). There was no conclusive evidence of any relationship between
238 alterations in MEP amplitude during pain, and alterations in N100, N45 and P60 amplitude
239 during pain (see supplementary material).

240 **Experiment 2 – Does acute pain alter cortical excitability or sensory potentials?**

241 Several studies have shown that a significant portion of TEPs do not reflect the direct
242 cortical response to TMS, but rather auditory potentials elicited by the “clicking” sound from
243 the TMS coil, and somatosensory potentials elicited by the “flicking” sensation on the skin of
244 the scalp (Biabani, Fornito, Mutanen, Morrow, & Rogasch, 2019; Chowdhury, et al., 2022;
245 Conde et al., 2019; Rocchi et al., 2021). Indeed, the signal at ~100ms post-TMS from
246 Experiment 1 may reflect an auditory N100 response. As it is extremely challenging to isolate
247 and filter these auditory and somatosensory evoked potentials using pre-processing pipelines,
248 masking methods have been used to suppress these sensory inputs, (Ilmoniemi & Kičić,
249 2010; Massimini et al., 2005). However recent studies have shown that even when these
250 methods are used, sensory contamination of TEPs is still present, as shown by commonalities
251 in the signal between active and sensory sham conditions that mimic the
252 auditory/somatosensory aspects of real TMS (Biabani et al., 2019; Conde et al., 2019; Rocchi
253 et al., 2021). This has led many leading authors (Biabani et al., 2019; Conde et al., 2019) to

254 recommend the use of sham conditions to control for sensory contamination. To separate the
255 direct cortical response to TMS from sensory evoked activity, Experiment 2 (n = 10) included
256 a sham TMS condition that mimicked the auditory/somatosensory aspects of active TMS to
257 determine whether any alterations in the TEP peaks in response to pain were due to changes
258 in sensory evoked activity associated with TMS, as opposed to changes in cortical
259 excitability. A similar design was used to Experiment 1, with the inclusion of a sham TMS
260 condition within the pre-pain and pain blocks, and exclusion of the post-pain block, since the
261 aim was to identify the source of the pain effect from Experiment 1. The sham TMS
262 condition was similar to a recent study (Gordon et al., 2021), involving the delivery of the
263 TMS coil rotated 90 degrees to the scalp to simulate the auditory component associated with
264 real TMS, and concurrent electrical stimulation beneath a sham coil to simulate the
265 somatosensory component associated with real TMS (see Figure 7A).

266 Figure 7B shows the grand average TEPs, scalp topographies and estimated source
267 activity for active and sham TMS, across pre-pain and pain conditions. Figure 8 shows the
268 mean TEP waveform for the frontocentral and parietal-occipital clusters identified from
269 Experiment 1, across active and sham conditions. There was moderate evidence that the
270 amplitude of the N45 peak was increased during pain vs. pre-pain blocks for active TMS
271 ($BF_{10} = 3.26$), and moderate evidence for no difference between pain and pre-pain blocks for
272 sham TMS ($BF_{10} = 0.309$). When comparing pain and pre-pain blocks, there was,
273 respectively, moderate and anecdotal evidence for no alterations in the frontocentral N100 for
274 active ($BF_{10} = 0.31$) and sham TMS ($BF_{10} = 0.42$). There was anecdotal evidence for no
275 alteration in the parietal occipital P60 for both active ($BF_{10} = 0.786$) and sham TMS ($BF_{10} =$
276 0.42). Overall, the results showed that the N45 peak was altered in response to pain for active
277 but not sham TMS, suggesting the experience of pain led to an alteration in the excitability of
278 the cortex, and not the auditory/somatosensory aspects of TMS.

279 **Experiment 3 – Does acute pain alter cortical excitability or reafferent muscle activity?**

280 Previous studies have shown that a significant portion of the TEP peaks at 45 and
281 60ms post-TMS reflect reafferent feedback from the muscle twitch in response to
282 suprathreshold TMS applied over M1. This comes from MRI-informed EEG studies showing
283 source localization of the N45 and P60 peaks to the somatosensory areas, as well as
284 correlations between MEP amplitude and N45/P60 amplitude (Ahn & Fröhlich, 2021;
285 Petrichella, Johnson, & He, 2017). Indeed, Experiments 1 and 2 also showed localization of
286 the N45 and P60 to sensorimotor areas. As such, Experiment 3 recruited a further ten
287 participants to determine whether the pain-induced increase in the N45 peak was due to
288 stronger reafferent feedback from muscle twitches. A design similar to Experiment 1 was
289 used, with the inclusion of a subthreshold TMS condition (90% RMT) within the pre-pain
290 and pain blocks.

291 Figure 9 shows the grand average TEPs, scalp topographies and estimated source
292 activity for supra- and subthreshold TMS, across pre-pain and pain blocks. Figure 10 shows
293 the mean TEP waveform for the frontocentral and parietal-occipital clusters identified from
294 Experiment 1, across suprathreshold and subthreshold TMS conditions. When comparing the
295 pain with pre-pain blocks, there was moderate evidence that the frontocentral N45 was
296 increased during subthreshold TMS ($BF_{10} = 3.05$) and suprathreshold TMS ($BF_{10} = 3.01$).
297 When comparing pain with pre-pain blocks, there was anecdotal evidence for no alterations
298 in the frontocentral N100 peak during suprathreshold TMS ($BF_{10} = 0.42$) and subthreshold
299 TMS ($BF_{10} = 0.36$). When comparing pain with pre-pain blocks, there was anecdotal
300 evidence for an increase in the parietal occipital P60 peak during suprathreshold TMS ($BF_{10} =$
301 2.71) and anecdotal evidence for no alteration in the P60 peak during subthreshold TMS
302 ($BF_{10} = 0.72$). Overall, there was evidence that that the N45 peak was altered in response to

303 both supra- and subthreshold TMS, suggesting the pain-induced increase in the N45 peak was
304 not a result of stronger reafferent feedback from the muscle twitches.

305

306 Discussion

307 The present study determined whether acute experimental pain induces alterations in
308 cortical inhibitory and/or facilitatory activity observed in TMS-evoked potentials. Across
309 three experiments, there was Bayesian evidence (varying between moderate to very strong)
310 for an increase in the amplitude of the N45 peak during painful stimuli compared to a non-
311 painful baseline. Experiment 1 showed very strong evidence that a larger increase in the N45
312 peak in response to pain was correlated with higher pain ratings. Experiment 2 showed that
313 the increase in the N45 peak during pain was not a result of alterations in sensory potentials
314 associated with the TMS pulses, but rather, changes in cortical excitability. Experiment 3
315 showed that the increase in the N45 peak was not a result of stronger reafferent feedback
316 from muscle twitches evoked by TMS during painful stimuli. While Experiment 1 showed
317 moderate evidence for an increase in N100 and P60 peaks during pain relative to pre-pain
318 baseline, this was not replicated in the follow-up experiments. Experiment 1 showed
319 anecdotal evidence for group-level alterations in MEP amplitude during pain, however there
320 was very strong evidence that a larger reduction in MEP amplitude during pain was
321 correlated with lower pain ratings.

322 Increased GABAergic activity during tonic pain

323 This study is the first to use TMS-EEG methodology to examine the direct cortical
324 response to acute pain, extending previous studies that have used TMS to measure MEPs in
325 response to pain (Chowdhury, et al., 2022). The key finding was an increase in the amplitude
326 of the N45 peak in response to pain. This result was replicated across three experiments,
327 providing robust evidence for the effect. Furthermore, we accounted for major confounds that
328 have caused significant data interpretation issues in the TMS-EEG literature in recent years,

329 namely the contamination of TEPs by sensory potentials associated with TMS pulses
330 (Biabani et al., 2019; Chowdhury, Rogasch, et al., 2022) and the presence of reafferent
331 feedback from muscle twitches (Ahn & Fröhlich, 2021).

332 The finding of a reliable increase in the amplitude of the N45 peak during pain
333 suggests a role for GABA_A neurotransmission in pain processing, as previous work has
334 shown that the amplitude of the N45 peak is increased in response to GABA_A agonists
335 (Premoli et al., 2014). Our source reconstruction results suggest that around this timepoint,
336 the current density was stronger in the sensorimotor area, consistent with the idea that the
337 N45 peak reflects GABAergic activity within the sensorimotor cortex (Farzan & Bortoletto,
338 2022). While it has been shown that reafferent muscle activity also contributes to the N45
339 peak (Ahn & Fröhlich, 2021), Experiment 3 showed that pain increased the amplitude of the
340 N45 peak even during subthreshold TMS. Taken together, these findings suggest that the
341 increased amplitude of the N45 peak in response to pain reflects an increase in GABAergic
342 activity within the sensorimotor cortex.

343 GABAergic neurons play a critical role in pain-related brain networks (Barr et al.,
344 2013; Ong, Stohler, & Herr, 2019). They are involved in the generation of gamma
345 oscillations (Buzsáki & Wang, 2012), which have been strongly implicated in pain perception
346 (Barr et al., 2013; Li, Zhang, Zeng, Zhao, & Hu, 2023). Indeed, previous work has shown an
347 increase in gamma oscillations in response to painful thermal stimuli comparable to the
348 present study, across a wide range of brain regions such as the prefrontal (Schulz et al., 2015)
349 and sensorimotor cortices (Gross, Schnitzler, Timmermann, & Ploner, 2007). It is therefore
350 possible that increases in the N45 peak during pain reflect increased sensorimotor gamma
351 oscillations. Further multimodal work is required to confirm this finding.

352 While our findings are consistent with some studies that show increases in
353 GABAergic activity in response to pain (Gross et al., 2007; Kupers, Danielsen, Kehlet,

354 Christensen, & Thomsen, 2009; Schulz et al., 2015), other studies have also reported reduced
355 GABAergic activity in response to experimental pain (Cleve, Gussew, & Reichenbach, 2015;
356 De Matos, Hock, Wyss, Ettlin, & Brügger, 2017). Differences between studies can be
357 attributed to the duration of the noxious stimulus (tonic pain lasting several seconds/minutes
358 vs. transient pain stimuli lasting <1second). Indeed, pooled data have shown that the cerebral
359 response to pain is highly dependent on the duration of the painful stimuli, as the adaptive
360 response (to suppress or increase cortical activity) changes depending on the duration of pain
361 (Chowdhury, et al., 2022). This highlights the need for further work to replicate our findings
362 using different durations of experimental and clinical pain.

363 Another finding of Experiment 1 was the increase in the amplitude of N100 peak, a
364 marker of GABA_B neurotransmission (Premoli et al., 2014), and the parietal-occipital P60
365 peak, a marker of glutamatergic neurotransmission (Belardinelli et al., 2021). However, this
366 was not replicated in Experiments 2 and 3, potentially due to the smaller sample size.
367 Nonetheless, we encourage further investigations of alterations in these peaks during pain,
368 particularly P60 peak, as several magnetic resonance spectroscopy studies have reported
369 increases in glutamate concentration during experimental pain (Archibald et al., 2020).

370 **Predicting individual differences in pain using TEPs**

371 Experimental pain models are useful tools to explore brain measures that may predict
372 individual differences in pain sensitivity, with an ultimate goal of determining whether such
373 measures explain why some people develop chronic pain. Experiment 1 showed that higher
374 pain ratings were associated with a larger increase in the N45 peak during pain. This analysis
375 was not conducted in Experiments 2 and 3 due to smaller sample sizes and given the primary
376 aims of Experiments 2 and 3 were to isolate the source of the group-level effect. Nonetheless,
377 our results suggest that the N45 peak is a potential marker of sensorimotor GABAergic
378 activity and may be associated with individual differences in pain sensitivity. This is

379 consistent with other studies measuring GABAergic responses to pain, showing associations
380 between higher pain sensitivity and larger sensorimotor gamma oscillations (Barr et al., 2013)
381 and higher left somatosensory cortical GABA laterality (Niddam, Wang, & Tsai, 2021).
382 However, the direction of this relationship likely depends on the duration of pain
383 (Chowdhury, et al., 2022). Our results have implications for understanding the development
384 and maintenance of chronic pain. Further TMS-EEG studies are required to determine
385 whether the N45 peak is altered in chronic pain populations and whether the N45 peak can
386 explain why some individuals in the acute stages of pain transition to chronic pain.

387 **The TEP vs. MEP response to pain**

388 The present study showed that a larger reduction in MEP amplitude during pain was
389 correlated with lower pain ratings, consistent with a recent systematic review (Chowdhury et
390 al., 2022) and the idea that reduced MEP amplitude is an adaptive mechanism that restricts
391 movement in the pain-afflicted area, to protect the area from further pain and injury (Hodges
392 & Tucker, 2011). The novelty of this study was the use of an experimental heat pain
393 paradigm that has not yet been used in combination with TMS research, and a paradigm that
394 controls for non-painful somatosensory stimulation.

395 The finding of a pain-induced increase in the amplitude of the N45 peak, which
396 indexes GABA_A receptor activity, is consistent with TMS research showing pain-induced
397 increases in short-interval intracortical inhibition (SICI) (Salo, Vaalto, Koponen, Nieminen,
398 & Ilmoniemi, 2019; Schabrun & Hodges, 2012). SICI refers to the reduction in MEP
399 amplitude to a TMS pulse that is preceded 1-5ms by a subthreshold pulse, with this reduction
400 believed to be mediated by GABA_A neurotransmission (Kujirai et al., 1993). Some studies
401 have reported associations between SICI and the TEP N45 peak (Leodori et al., 2019; Rawji,
402 Kaczmarczyk, Rocchi, Rothwell, & Sharma, 2019), suggesting the two may share common
403 neurophysiological mechanisms. However, we also found that a larger reduction in MEP

404 amplitude during pain was associated with less pain, while a larger increase in the TEP N45
405 peak during pain was associated with stronger pain ratings, suggesting that inhibitory
406 processes mediating MEPs and the TEP N45 peak during pain are distinct. Further work is
407 required to disentangle the relationship between corticomotor excitability measured by MEPs
408 and cortical activity measured by TEPs.

409 **Study limitations**

410 Some methodological limitations should be noted. Firstly, while there was no
411 conclusive evidence for a difference in pain ratings between the six thermal stimuli of the
412 pain block, there was evidence for fluctuations in pain ratings during each painful stimulus.
413 This suggests that the perceived pain intensity was not stable across 40 seconds, which may
414 have introduced noise in the TEP data. Future studies could use pain paradigms that can more
415 effectively maintain a constant level of pain e.g., hypertonic saline infusion paradigms
416 (Svensson, Cairns, Wang, & Arendt-Nielsen, 2003). Secondly, the use of verbal pain ratings
417 prevented the characterisation of pain on a finer time scale. However, verbal ratings were
418 used to eliminate potential contamination of MEPs introduced by using the hand for
419 providing pain rating. Thirdly, the increased N45 peak amplitude in response to pain may
420 reflect increased alertness/arousal during pain. However, a recent study showed that higher
421 alertness is associated with reduced TEP amplitude (Noreika et al., 2020), suggesting the
422 increase in the N45 peak amplitude is not related to pain-induced arousal. Lastly, future
423 research should consider replicating our experiment using intermixed pain and no pain
424 blocks, as opposed to fixed pre-pain and pain blocks, to control for order effects i.e. the
425 explanation that successive thermal stimuli applied to the skin results an increase in the N45
426 peak, regardless of whether the stimuli are painful or not. However, we note that there was no
427 conclusive evidence for a difference in N45 peak amplitude between pre-pain and post-pain

428 conditions of Experiment 1 (Supplementary Figure 1), suggesting it is unlikely that the
429 observed effects were an artefact of time.

430 **Conclusion**

431 This study is the first to use TMS-EEG methodology to examine alterations in cortical
432 activity in direct response to acute pain. Findings across three experiments suggest that tonic
433 heat pain leads to an increase in the amplitude of the frontocentral TEP N45 peak (associated
434 with GABAergic neurotransmission), and that larger increases in this peak are associated
435 with higher pain ratings. The findings suggest that TEP indices of GABAergic
436 neurotransmission have the potential as predictive markers of pain severity.

437

438

439

440

441

442

443

444

445

446

447

448

449

450

451

452

453

Materials and Methods

454 **Participants**

455 Experiment 1 consisted of 29 healthy participants (18 males, 11 females, mean age;
456 26.24 ± 5.5). Participants were excluded if they had a history of chronic pain condition or
457 any current acute pain, any contraindication to TMS such as pregnancy, mental implants in
458 the skull, seizure, or if they reported a history of neurological or psychiatric conditions, or
459 were taking psychoactive medication. Participants completed a TMS safety screen (Rossi,
460 Hallett, Rossini, Pascual-Leone, & Group, 2009). Procedures adhered to the Declaration of
461 Helsinki and were approved by the human research ethics committee of UNSW (HC200328).
462 All participants provided informed written consent.

463 The sample size calculation was done in G*power 3.1.9.7 with 80% power. As there
464 were no prior TMS-EEG studies, we used pooled data from our systematic review on TMS
465 studies (Chowdhury et al., 2022) showing that the weighted effect size of changes in MEP
466 amplitude in response to tonic experimental pain was 0.56. Using this value, 28 participants
467 were required to detect a significant difference between pain and pre-pain blocks.

468 To determine the sample size of Experiments 2 and 3, we computed the effect sizes of
469 the N45, P60 and N100 changes (pain vs. prepain) from Experiment 1 (Cohen's $d_{RM} = 1.76$,
470 0.99, 0.83 for N45, P60 and N100 respectively). With a power of 80%, the required sample
471 size was 4-11 participants to detect a significant difference. Experiment 2 recruited a further
472 ten healthy participants (four males, six females, mean age: 26.8 ± 5.9) and Experiment 3
473 consisted of ten healthy participants (four males, six females, mean age: 28 ± 5.9).

474 **Experimental protocol**

475 Participants were seated comfortably in a shielded room. They viewed a fixation
476 cross to minimise eye movements. TMS was applied to left M1 while participants wore an
477 EEG cap containing 63 scalp electrodes to record TEPs. Surface electromyographic (EMG)

478 electrodes were placed over the distal region of the right ECRB to record MEPs. EMG
479 signals were amplified (x 1000) and filtered (16 to 1000Hz), and digitally sampled at 2000
480 Hz (Spike2, CED). A thermode was attached over the proximal region of the right ECRB in
481 close proximity to the EMG electrodes (Figure 1). The TMS coil was covered in a layer of
482 foam (5mm thickness) to minimize decay artefacts (Rogasch et al., 2017). Participants also
483 wore both foam earplugs and headphones to reduce any potential discomfort from the TMS
484 click. Auditory masking was not used. Instead, auditory evoked potentials resulting from the
485 TMS click sound were controlled for in Experiment 2.

486 The protocol for each experiment is illustrated in Figure 2 (Furman et al., 2020;
487 Granot et al., 2006). In Experiment 1, participants experienced three blocks of thermal
488 stimuli, in chronological order: pre-pain, pain, and post-pain block. Each block consisted of
489 multiple thermal stimuli delivered 40s at a time during which suprathreshold (110% RMT)
490 TMS measurements and verbal pain ratings were obtained. The thermode commenced at a
491 baseline temperature of 32°C. The pre-pain and post-pain blocks consisted of six thermal
492 stimuli delivered at the warm threshold (the temperature that led to any detectable change in
493 skin temperature from baseline). In the pain block, six thermal stimuli were delivered at
494 46°C, which has been shown to produce lasting pain with a mean rating of ~5/10 (Furman et
495 al., 2020). Given we were interested in the individual relationship between pain and
496 excitability changes, the fixed temperature of 46°C ensured larger variability in pain ratings
497 as opposed to calibrating the temperature of the thermode for each participant (Adamczyk et
498 al., 2022). The inclusion of blocks with warm stimuli allowed for control for changes in
499 cortical excitability due to non-painful somatosensory stimulation.

500 The protocol for Experiment 2 and 3 were identical to Experiment 1 with two
501 differences: the exclusion of the post-pain block (as the aim was to disentangle the source of
502 the pain vs. pre-pain effect from Experiment 1) and the inclusion of a sham TMS condition

503 (Experiment 2) or subthreshold (90% RMT) TMS (Experiment 3) intermixed within both the
504 pre-pain and pain blocks.

505

506 **Electrical stimulation setup (Experiment 2 Only)**

507 Electrical stimulation was based on previous studies attempting to simulate the
508 somatosensory component of active TMS (Chowdhury et al., 2022; Gordon et al., 2022;
509 Rocchi et al., 2021). Prior to EEG setup, 8mm Ag/AgCl electrodes were placed directly over
510 the scalp. “Snap on” lead wires were then clipped in place and connected to the electrical
511 stimulator (Digitimer DS7AH, Digitimer Ltd., UK). To keep the electrodes and lead wires
512 firmly in position, participants were fitted with a tight netted wig cap, which sat on top of the
513 electrodes but underneath the EEG cap. Consistent with previous research (Chowdhury,
514 Rogasch, et al., 2022; Rocchi et al., 2021), and to minimize EEG artefacts caused by
515 electrical stimulation, the stimulating electrodes were not placed directly underneath the EEG
516 electrodes. Rather, stimulating electrodes were positioned in the middle of the EEG electrode
517 cluster located in closest proximity to the motor hotspot. This roughly corresponded to an
518 anode position between FC1 and FC3 and a cathode position between C1 and C3. Scalp
519 electrical stimulation was delivered using a 200 μ s square wave via with a compliance of
520 200V.

521

522 **Electroencephalography**

523 EEG was recorded using a DC-coupled, TMS-compatible amplifier (ActiChamp Plus,
524 Brain Products, Germany) at a sampling rate of 25000 Hz. Signals were recorded from 63
525 TMS-compatible active electrodes (6mm height, 13mm width), embedded in an elastic cap
526 (ActiCap, Brain Products, Germany), in line with the international 10-10 system. Active
527 electrodes result in similar TEPs (both magnitude and peaks) to more commonly used passive

528 electrodes (Mancuso et al., 2021). There is also evidence that active electrodes have higher
529 signal quality than passive electrodes at higher impedance levels (Laszlo, Ruiz-Blondet,
530 Khalifian, Chu, & Jin, 2014). Recordings were referenced online to 'FCz' and the ground
531 electrode placed on 'FPz'. Electrolyte gel was used to reduce electrode impedances below
532 ~5kOhms. Online TEP monitoring was not available with the EEG software.

533 **Transcranial magnetic stimulation.**

534 Single, monophasic stimuli were delivered using a Magstim unit (Magstim Ltd., UK)
535 and 70mm figure-of-eight flat coil. The coil was oriented at 45° to the midline, inducing a
536 current in the posterior-anterior direction. The scalp site that evoked the largest MEP
537 measured at the ECRB ('hotspot') was determined and marked. The RMT was determined
538 using the TMS motor thresholding assessment tool, which estimates the TMS intensity
539 required to induce an MEP of 50 microvolts with a 50% probability using maximum
540 likelihood parametric estimation by sequential testing (Awiszus, 2003; Awiszus & Borckardt,
541 2011). This method has been shown to achieve the accuracy of methods such as the Rossini-
542 Rothwell method (Rossini et al., 1994; Rothwell et al., 1999) but with fewer pulses (Qi, Wu,
543 & Schweighofer, 2011; Silbert, Patterson, Pevcic, Windnagel, & Thickbroom, 2013). The test
544 stimulus intensity was set at 110% RMT to concurrently measure MEPs and TEPs during
545 pre-pain, pain and post-pain blocks.

546 **Thermal pain**

547 Thermal stimuli were delivered over the proximal region of the right ECRB using a
548 contact heat stimulator (27-mm diameter Medoc Pathway CHEPS Peltier device; Medoc
549 Advanced Medical Systems Ltd). Pain ratings were obtained after each TMS pulse using a
550 verbal rating scale (0 = no pain, and 10 = most pain imaginable). Verbal ratings were
551 collected rather than pain ratings provided on the computer by hand to avoid contamination

552 of MEP measures from motor processes of hand movements. Verbal pain ratings have been
553 shown to yield excellent test-retest reliability (Alghadir, Anwer, Iqbal, & Iqbal, 2018).

554 **Quantitative sensory testing**

555 Warmth, cold and pain thresholds were assessed in line with a previous study
556 (Furman et al., 2020). With the baseline temperature set at a neutral skin temperature of
557 32°C, participants completed three threshold tests: to report when they felt a temperature
558 increase (warmth detection threshold) (Furman et al., 2020), to report when they felt a
559 temperature decrease (cool detection threshold) (Furman et al., 2020); 3) to report when an
560 increasing temperature first became painful (heat pain threshold) (Furman et al., 2020). A
561 total of three trials was conducted for each test to obtain an average, with an interstimulus
562 interval of six seconds (Furman et al., 2020). The sequence of cold, warmth and pain
563 threshold was the same for all participants. Participants provided feedback for each trial by
564 pressing a button (with their left hand) on a hand-held device connected to the Medoc
565 Pathway. Temperatures were applied with a rise/decrease rate of 1°C/s and return rate of
566 2°C/s (initiated by the button click).

567

568 **Matching task (Experiment 2 only)**

569 As the aim of Experiment 2 was to perceptually match the somatosensory aspects of
570 active and sham TMS, a 2-Alternative Forced Choice task was used to determine the
571 electrical stimulation intensity that led to a similar flicking sensation to active TMS
572 (Chowdhury, et al., 2022). Participants received either electrical stimulation or active TMS in
573 a randomized order and were asked whether the first or second stimulus led to a stronger flick
574 sensation. The electrical stimulation intensity was then increased or decreased until
575 participants could no longer judge the first or second stimulus as stronger. This intensity was
576 then applied during the test blocks.

577 **Test blocks**

578 **Experiment 1.** The temperature of the thermode commenced at a neutral skin
579 temperature (32°C). Participants were exposed to 18 sustained thermal stimuli with a 20
580 second interstimulus interval. For each thermal stimulus, a single temperature (rise rate of 1
581 °C/s, return rate of 2 °C/s) was applied over the proximal region of the ECRB for 40 seconds.
582 Thermal stimuli 1-6 (pre-pain block) were delivered at the participant's individually
583 determined warmth detection threshold, Thermal stimuli 7-12 at 46 degrees, and Thermal
584 stimuli 13-18 again at the participant's warmth detection threshold. Participants were not
585 informed of the order of the warm and painful stimuli to minimize the influence of
586 expectation of pain on TEPs and MEPs. During each 40 second thermal stimulus, TMS
587 pulses were manually delivered, with a verbal pain rating score (0 = no pain, and 10 = worst
588 pain imaginable) obtained between pulses. To avoid contamination of TEPs by verbal ratings,
589 the subsequent TMS pulse was not delivered until the verbal rating was complete, and the
590 participant was cued by the experimenter to provide the pain rating after each pulse. As TMS
591 was delivered manually, there was no set interpulse interval. However, the 40 second thermal
592 stimulus duration allowed for 11 pulses for each thermal stimulus (hence 66 TMS pulses for
593 each of the pre-pain, pain and post-pain blocks), and 10 verbal pain ratings between each
594 TMS pulse (~ 4 seconds in between pain ratings). Current recommendations (Hernandez-
595 Pavon et al., 2023) suggest basing the number of TMS trials per condition on the key
596 outcome measure (e.g., TEP peaks vs. frequency measures) and based on previous test-retest
597 reliability studies. In our study the number of trials was based on a test-retest reliability study
598 by (Kerwin, Keller, Wu, Narayan, & Etkin, 2018) which showed that 60 TMS pulses
599 (delivered in the same run) was sufficient to obtain reliable TEP peaks (i.e., sufficient within-
600 individual concordance between the resultant TEP peaks of each trial).

601 **Experiment 2.** Participants were exposed to 24 sustained thermal stimuli (40 seconds
602 each). Thermal stimuli 1-6 and 7-12 consisted of warm stimuli (pre-pain block), while
603 Thermal stimuli 13-18 and 19-24 consisted of stimuli delivered at 46°C (pain block). Active
604 or sham TMS was delivered during either thermal stimuli 1-6 or 7-12, with the order of active
605 and sham randomly determined for each participant. The same applied for thermal stimuli 13-
606 18 and 19-24. The active and sham TMS conditions were similar to that used in a recent
607 TMS-EEG study (Gordon et al., 2021). Sham TMS involved the active TMS coil rotated 90
608 degrees to the scalp, and a sham coil (identical in shape/weight) placed underneath the active
609 coil and tangentially over the scalp. The active TMS coil was then triggered with the
610 electrical stimulation unit to simultaneously simulate the auditory and somatosensory
611 components of active TMS respectively. Active TMS involved the delivery of the TMS coil
612 placed tangentially over the scalp, and the sham TMS coil above the active coil rotated 90
613 degrees to the scalp (see Figure 9). The design allowed for 11 pulses for each thermal
614 stimulus and ten pain ratings (hence 66 TMS pulses for active pre-pain, sham pre-pain, active
615 pain and sham pain blocks).

616 **Experiment 3.** Participants were exposed to 24 sustained thermal stimuli (40 seconds
617 each). Thermal stimuli 1-6 and 7-12 consisted of warm stimuli (pre-pain block), while
618 thermal stimuli 13-18 and 19-24 consisted of thermal stimuli delivered at 46°C (pain block).
619 Suprathreshold or subthreshold TMS (90% RMT) was delivered during either thermal stimuli
620 1-6 or 7-12, with the order of supra- and subthreshold TMS randomly determined for each
621 participant. The same applied for thermal stimuli 13-18 and 19-24. In addition to the pain
622 rating in between TMS pulses, we collected a second rating for warmth of the thermal
623 stimulus (0 = neutral, 10 = very warm) to confirm that the participants felt some difference in
624 sensation relative to baseline during the pre-pain block. This data is presented in the
625 supplementary material. Overall, the design allowed for 11 pulses for each thermal stimulus

626 and ten pain/warmth ratings (hence 66 TMS pulses for suprathreshold pre-pain, subthreshold
627 pre-pain, suprathreshold pain and subthreshold pain blocks).

628

629 **Data processing**

630 ***Motor evoked potentials.*** The amplitude of each MEP was determined using a custom
631 MATLAB script. The onsets and offsets of the MEPs were manually determined for each
632 trial. In some participants, background EMG activity was observed due to placement of the
633 thermode close to the EMG electrodes, which can influence MEP amplitude (Ruddy et al.,
634 2018). To account for this, MEP amplitude was calculated by subtracting the root mean
635 square (RMS) of background EMG noise from the RMS of the MEP window using a fixed
636 window between 55 and 5ms before the TMS pulse (Chowdhury et al., 2023; Schabrun et al.,
637 2017; Tsao et al., 2011).

638 ***TMS-evoked potentials.*** Pre-processing of the TEPs was completed using EEGLAB
639 (Delorme & Makeig, 2004) and TESA (Rogasch et al., 2017) in MATLAB (R2021b, The
640 Math works, USA), and based on previously described methods (Chowdhury et al., 2022;
641 Mutanen et al., 2018; Rogasch et al., 2017). First, bad channels were removed. The period
642 between -5 and ~14ms after the TMS pulse was removed and interpolated using the ARFIT
643 function for continuous data (Neumaier & Schneider, 2001; Schneider & Neumaier, 2001).
644 The exact interval was based on the duration of decay artefacts. Data was epoched 1000ms
645 before and after the TMS pulse, and baseline corrected between -1000 and -5ms before the
646 TMS pulse. Noisy epochs were identified via the EEGLAB auto-trial rejection function
647 (Delorme, Sejnowski, & Makeig, 2007) and then visually confirmed. The fastICA algorithm
648 with auto-component rejection used to remove eyeblink and muscle artefacts (Rogasch et al.,
649 2017). The source-estimation noise-discriminating (SOUND) algorithm was applied (Mutanen,
650 Biabani, Sarvas, Ilmoniemi, & Rogasch, 2020; Mutanen, Metsomaa, Liljander, & Ilmoniemi,

651 2018), which estimates and suppresses noise at each channel based on the most likely cortical
652 current distribution given the recording of other channels. This signal was then re-referenced
653 (to average). A band-pass (1-100Hz) and band-stop (48-52Hz) Butterworth filter was then
654 applied. Any lost channels were interpolated.

655 **Source localization.** Source localization of TEPs was conducted using Brainstorm
656 (Tadel, Baillet, Mosher, Pantazis, & Leahy, 2011). A template brain model (ICBM 152) was
657 co-registered with the TMS-EEG data. Noise estimation was used to determine sensor
658 weighting and regularization parameter of the current density construction. The forward
659 model involved use of the Symmetric Boundary Element Method with the head having 3
660 compartments of fixed conductivities, implemented in OpenMEEG software (Gramfort,
661 Papadopoulou, Olivi, & Clerc, 2010), and inverse model involved use of Minimum Norm
662 Estimations.

663 **Statistical Analysis**

664 Given we were interested in determining the evidence for pain altering TEP peaks in
665 certain conditions (e.g., active TMS) and pain not altering TEP peaks in other conditions
666 (sham TMS), we used a Bayesian approach as opposed to a frequentist approach, which
667 considers the strength of the evidence for the alternative vs. null hypothesis. Bayesian
668 inference was used to analyse the data using JASP software (Version 0.12.2.0, JASP Team,
669 2020). Bayes factors were expressed as BF_{10} values, where BF_{10} 's of 1-3, 3-10, 10-30 and 30-
670 100 indicated "weak", "moderate", "strong" and "very strong" evidence for the alternative
671 hypothesis, while BF_{10} 's of 1/3-1, 1/10-1/3, 1/30-1/10 and 1/100-1/30 indicated "anecdotal",
672 "moderate", "strong" and "very strong" evidence in favour of the null hypothesis (van Doorn
673 et al., 2021).

674 **Pain ratings.** A 6 (thermal stimulus number: 1-6) x 10 (timepoint:1-10) Bayesian
675 repeated measures ANOVA with default priors in JASP (r scale fixed effects = .5, r scale

676 random effects = 1, r scale covariates = .354) was conducted on the pain ratings during the
677 pain block. This was to assess differences in pain ratings between the six painful stimuli and
678 whether pain ratings differed between the timepoints of each painful stimulus.

679 **MEPs.** A Bayesian one-way repeated measures ANOVA with default priors in JASP
680 was performed to assess differences in MEP amplitudes between pre-pain, pain and post-pain
681 blocks of Experiment 1. As there is now increasing emphasis placed on investigating the
682 individual level relationship between changes in cortical excitability and pain and not only
683 the group level effect, (Chowdhury et al., 2022; Seminowicz et al., 2018; Seminowicz,
684 Thapa, & Schabrun, 2019; Summers et al., 2019) we also investigated the correlations
685 between pain ratings and changes in MEP (and TEP) amplitude. A Bayesian correlation
686 analysis with default priors in JASP (stretched Beta prior width = 1) was run to determine
687 whether the change in mean MEP amplitude during pain (as a proportion of pre-pain) was
688 associated with the mean verbal pain rating score. Data were checked for assumptions of
689 normally distributed data using a Shapiro-Wilk test. Where assumptions were violated, data
690 were log-transformed.

691 **TEPs.** The grand-averaged signals for the pre-pain, pain and post-pain condition were
692 obtained. For Experiment 1, a cluster-based permutation analysis was used to compare
693 amplitude levels between pre-pain and pain, and pre-pain and post-pain, at each time-point
694 and for each electrode. For all experiments, the mean TEP waveform of any identified
695 clusters from Experiment 1 were plotted, and peaks (e.g., N15, P30, N45, P60, N100) were
696 identified using the TESA peak function (Rogasch et al., 2017). Any identified peaks were
697 then compared between conditions using Bayes paired sample t-tests with default priors in
698 JASP (Cauchy scale = .707). A Bayesian correlation analysis with default priors in JASP was
699 performed to determine whether the difference in identified peaks between pre-pain and pain
700 blocks was associated with the mean pain rating score. Data were checked for assumptions of

701 normally distributed data using a Shapiro-Wilk test. Where assumptions were violated, data
702 were log-transformed.

703

704 **Acknowledgements**

705 This work was supported by 1R61NS113269-01 from The National Institutes of Health to
706 DAS, SMS, and The Four Borders Foundation to DAS.

707

708

709

710

711

712

713

714

715

716

717

718

719

720

721

722

723

724

725

726

References

727 Adamczyk, W. M., Szikszay, T. M., Nahman-Averbuch, H., Skalski, J., Nastaj, J., Gouverneur, P., &
728 Luedtke, K. (2022). To calibrate or not to calibrate? A methodological dilemma in
729 experimental pain research. *The journal of Pain*, 23(11), 1823-1832.

730 Ahn, S., & Fröhlich, F. (2021). Pinging the brain with transcranial magnetic stimulation reveals
731 cortical reactivity in time and space. *Brain stimulation*, 14(2), 304-315.

732 Alghadir, A. H., Anwer, S., Iqbal, A., & Iqbal, Z. A. (2018). Test-retest reliability, validity, and
733 minimum detectable change of visual analog, numerical rating, and verbal rating scales for
734 measurement of osteoarthritic knee pain. *Journal of pain research*, 11, 851.

735 Apkarian, A. V. (2021). The Necessity of Methodological Advances in Pain Research: Challenges and
736 Opportunities. *Frontiers in Pain Research*, 2, 10.

737 Archibald, J., MacMillan, E. L., Graf, C., Kozlowski, P., Laule, C., & Kramer, J. L. K. (2020). Metabolite
738 activity in the anterior cingulate cortex during a painful stimulus using functional MRS.
739 *Scientific Reports*, 10(1), 19218. doi:10.1038/s41598-020-76263-3

740 Awiszus, F. (2003). TMS and threshold hunting. In *Supplements to Clinical neurophysiology* (Vol. 56,
741 pp. 13-23): Elsevier.

742 Awiszus, F., & Borckardt, J. (2011). TMS motor threshold assessment tool (MTAT 2.0). *Brain
743 Stimulation Laboratory, Medical University of South Carolina, USA*.

744 Bank, P. J., Peper, C., Marinus, J., Beek, P. J., & Van Hilten, J. (2013). Motor consequences of
745 experimentally induced limb pain: a systematic review. *European journal of pain*, 17(2), 145-
746 157.

747 Barr, M. S., Farzan, F., Davis, K. D., Fitzgerald, P. B., & Daskalakis, Z. J. (2013). Measuring GABAergic
748 inhibitory activity with TMS-EEG and its potential clinical application for chronic pain. *Journal
749 of Neuroimmune Pharmacology*, 8(3), 535-546.

750 Belardinelli, P., König, F., Liang, C., Premoli, I., Desideri, D., Müller-Dahlhaus, F., . . . Ziemann, U.
751 (2021). TMS-EEG signatures of glutamatergic neurotransmission in human cortex. *Scientific
752 Reports*, 11(1), 1-14.

753 Biabani, M., Fornito, A., Mutanen, T. P., Morrow, J., & Rogasch, N. C. (2019). Characterizing and
754 minimizing the contribution of sensory inputs to TMS-evoked potentials. *Brain stimulation*,
755 12(6), 1537-1552.

756 Brodbeck, V., Spinelli, L., Lascano, A. M., Wissmeier, M., Vargas, M.-I., Vulliemoz, S., . . . Seeck, M.
757 (2011). Electroencephalographic source imaging: a prospective study of 152 operated
758 epileptic patients. *Brain*, 134(10), 2887-2897. doi:10.1093/brain/awr243

759 Burns, E., Chipchase, L. S., & Schabrun, S. M. (2016). Primary sensory and motor cortex function in
760 response to acute muscle pain: A systematic review and meta-analysis. *European Journal of
761 pain*, 20(8), 1203-1213. doi:10.1002/ejp.859

762 Buzsáki, G., & Wang, X.-J. (2012). Mechanisms of gamma oscillations. *Annual review of neuroscience*,
763 35, 203.

764 Chang, W.-J., O'Connell, N. E., Beckenkamp, P. R., Alhassani, G., Liston, M. B., & Schabrun, S. M.
765 (2018). Altered primary motor cortex structure, organization, and function in chronic pain: a
766 systematic review and meta-analysis. *The journal of Pain*, 19(4), 341-359.

767 Che, X., Cash, R., Chung, S. W., Bailey, N., Fitzgerald, P. B., & Fitzgibbon, B. M. (2019). The
768 dorsomedial prefrontal cortex as a flexible hub mediating behavioral as well as local and
769 distributed neural effects of social support context on pain: A Theta Burst Stimulation and
770 TMS-EEG study. *Neuroimage*, 201, 116053.

771 Chowdhury, N. S., Chang, W.-J., Millard, S. K., Skippen, P., Bilska, K., Seminowicz, D. S., & Schabrun, S.
772 M. (2022). The Effect of Acute and Sustained Pain on Corticomotor Excitability: A Systematic
773 Review and Meta-analysis of group-and individual-level data. *The journal of Pain*.

774 Chowdhury, N. S., Rogasch, N. C., Chiang, A. K., Millard, S. K., Skippen, P., Chang, W.-J., . . . Schabrun,
775 S. M. (2022). The influence of sensory potentials on transcranial magnetic stimulation–
776 Electroencephalography recordings. *Clinical Neurophysiology*, 140, 98-109.

777 Cleve, M., Gussew, A., & Reichenbach, J. R. (2015). In vivo detection of acute pain-induced changes
778 of GABA+ and Glx in the human brain by using functional 1H MEGA-PRESS MR spectroscopy.
779 *Neuroimage*, 105, 67-75.

780 Conde, V., Tomasevic, L., Akopian, I., Stanek, K., Saturnino, G. B., Thielscher, A., . . . Siebner, H. R.
781 (2019). The non-transcranial TMS-evoked potential is an inherent source of ambiguity in
782 TMS-EEG studies. *Neuroimage*, 185, 300-312.

783 De Matos, N. M., Hock, A., Wyss, M., Ettlin, D. A., & Brügger, M. (2017). Neurochemical dynamics of
784 acute orofacial pain in the human trigeminal brainstem nuclear complex. *Neuroimage*, 162,
785 162-172.

786 Delorme, A., & Makeig, S. (2004). EEGLAB: an open source toolbox for analysis of single-trial EEG
787 dynamics including independent component analysis. *Journal of neuroscience methods*,
788 134(1), 9-21.

789 Delorme, A., Sejnowski, T., & Makeig, S. (2007). Enhanced detection of artifacts in EEG data using
790 higher-order statistics and independent component analysis. *Neuroimage*, 34(4), 1443-1449.

791 Dubé, J. A., & Mercier, C. (2011). Effect of pain and pain expectation on primary motor cortex
792 excitability. *Clinical Neurophysiology*, 122(11), 2318-2323.

793 Farzan, F., & Bortoletto, M. (2022). Identification and verification of a 'true' TMS evoked potential in
794 TMS-EEG. *Journal of neuroscience methods*, 109651.

795 Farzan, F., Vernet, M., Shafi, M. M., Rotenberg, A., Daskalakis, Z. J., & Pascual-Leone, A. (2016).
796 Characterizing and modulating brain circuitry through transcranial magnetic stimulation
797 combined with electroencephalography. *Frontiers in neural circuits*, 10, 73.

798 Frömer, R., Maier, M., & Abdel Rahman, R. (2018). Group-level EEG-processing pipeline for flexible
799 single trial-based analyses including linear mixed models. *Frontiers in neuroscience*, 12, 48.

800 Furman, A. J., Prokhorenko, M., Keaser, M. L., Zhang, J., Chen, S., Mazaheri, A., & Seminowicz, D. A.
801 (2020). Sensorimotor peak alpha frequency is a reliable biomarker of prolonged pain
802 sensitivity. *Cerebral Cortex*, 30(12), 6069-6082.

803 Gordon, P. C., Jovellar, D. B., Song, Y., Zrenner, C., Belardinelli, P., Siebner, H. R., & Ziemann, U.
804 (2021). Recording brain responses to TMS of primary motor cortex by EEG—utility of an
805 optimized sham procedure. *Neuroimage*, 118708.

806 Gramfort, A., Papadopoulou, T., Olivi, E., & Clerc, M. (2010). OpenMEEG: opensource software for
807 quasistatic bioelectromagnetics. *Biomedical engineering online*, 9(1), 1-20.

808 Granot, M., Granovsky, Y., Sprecher, E., Nir, R.-R., & Yarnitsky, D. (2006). Contact heat-evoked
809 temporal summation: tonic versus repetitive-phasic stimulation. *Pain*, 122(3), 295-305.

810 Gross, J., Schnitzler, A., Timmermann, L., & Ploner, M. (2007). Gamma oscillations in human primary
811 somatosensory cortex reflect pain perception. *PLoS biology*, 5(5), e133.

812 Hernandez-Pavon, J. C., Veniero, D., Bergmann, T. O., Belardinelli, P., Bortoletto, M., Casarotto, S., . . .
813 Julkunen, P. (2023). TMS combined with EEG: Recommendations and open issues for data
814 collection and analysis. *Brain Stimulation*.

815 Hodges, P. W., & Tucker, K. (2011). Moving differently in pain: A new theory to explain the
816 adaptation to pain. *Pain*, 152(SUPPL.3), S90-S98. doi:10.1016/j.pain.2010.10.020

817 Ilmoniemi, R. J., & Kičić, D. (2010). Methodology for combined TMS and EEG. *Brain Topography*, 22,
818 233-248.

819 Kallioniemi, E., & Daskalakis, Z. J. (2022). Identifying novel biomarkers with TMS-EEG -
820 Methodological possibilities and challenges. *J Neurosci Methods*, 377, 109631.
821 doi:10.1016/j.jneumeth.2022.109631

822 Kerwin, L. J., Keller, C. J., Wu, W., Narayan, M., & Etkin, A. (2018). Test-retest reliability of
823 transcranial magnetic stimulation EEG evoked potentials. *Brain stimulation*, 11(3), 536-544.
824 doi:<https://doi.org/10.1016/j.brs.2017.12.010>

825 Kujirai, T., Caramia, M., Rothwell, J. C., Day, B., Thompson, P., Ferbert, A., . . . Marsden, C. D. (1993).
826 Corticocortical inhibition in human motor cortex. *The Journal of Physiology*, 471(1), 501-519.
827 Kupers, R., Danielsen, E. R., Kehlet, H., Christensen, R., & Thomsen, C. (2009). Painful tonic heat
828 stimulation induces GABA accumulation in the prefrontal cortex in man. *Pain*, 142(1-2), 89-
829 93.
830 Laszlo, S., Ruiz-Blondet, M., Khalifian, N., Chu, F., & Jin, Z. (2014). A direct comparison of active and
831 passive amplification electrodes in the same amplifier system. *Journal of neuroscience*
832 *methods*, 235, 298-307.
833 Leodori, G., Thirugnanasambandam, N., Conn, H., Popa, T., Berardelli, A., & Hallett, M. (2019).
834 Intracortical inhibition and surround inhibition in the motor cortex: a TMS-EEG study.
835 *Frontiers in neuroscience*, 13, 612.
836 Li, Z., Zhang, L., Zeng, Y., Zhao, Q., & Hu, L. (2023). Gamma-band oscillations of pain and nociception:
837 A systematic review and meta-analysis of human and rodent studies. *Neuroscience &*
838 *Biobehavioral Reviews*, 146, 105062. doi:<https://doi.org/10.1016/j.neubiorev.2023.105062>
839 Mancuso, M., Sveva, V., Cruciani, A., Brown, K., Ibáñez, J., Rawji, V., . . . Rothwell, J. (2021).
840 Transcranial evoked potentials can be reliably recorded with active electrodes. *Brain*
841 *Sciences*, 11(2), 145.
842 Massimini, M., Ferrarelli, F., Huber, R., Esser, S. K., Singh, H., & Tononi, G. (2005). Breakdown of
843 cortical effective connectivity during sleep. *Science*, 309(5744), 2228-2232.
844 Michel, C. M., & Brunet, D. (2019). EEG source imaging: a practical review of the analysis steps.
845 *Frontiers in Neurology*, 10, 325.
846 Mutanen, T. P., Biabani, M., Sarvas, J., Ilmoniemi, R. J., & Rogasch, N. C. (2020). Source-based
847 artifact-rejection techniques available in TESA, an open-source TMS-EEG toolbox. *Brain*
848 *Stimulation: Basic, Translational, and Clinical Research in Neuromodulation*, 13(5), 1349-
849 1351.
850 Mutanen, T. P., Metsomaa, J., Liljander, S., & Ilmoniemi, R. J. (2018). Automatic and robust noise
851 suppression in EEG and MEG: The SOUND algorithm. *Neuroimage*, 166, 135-151.
852 Neumaier, A., & Schneider, T. (2001). Estimation of parameters and eigenmodes of multivariate
853 autoregressive models. *ACM Transactions on Mathematical Software (TOMS)*, 27(1), 27-57.
854 Niddam, D. M., Wang, S.-J., & Tsai, S.-Y. (2021). Pain sensitivity and the primary sensorimotor
855 cortices: a multimodal neuroimaging study. *Pain*, 162(3), 846-855.
856 Ong, W.-Y., Stohler, C. S., & Herr, D. R. (2019). Role of the Prefrontal Cortex in Pain Processing.
857 *Molecular Neurobiology*, 56(2), 1137-1166. doi:10.1007/s12035-018-1130-9
858 Petrichella, S., Johnson, N., & He, B. (2017). The influence of corticospinal activity on TMS-evoked
859 activity and connectivity in healthy subjects: A TMS-EEG study. *PLoS one*, 12(4), e0174879.
860 Ploner, M., & May, E. S. (2018). Electroencephalography and magnetoencephalography in pain
861 research—current state and future perspectives. *Pain*, 159(2), 206-211.
862 Premoli, I., Castellanos, N., Rivolta, D., Belardinelli, P., Bajo, R., Zipser, C., . . . Ziemann, U. (2014).
863 TMS-EEG signatures of GABAergic neurotransmission in the human cortex. *Journal of*
864 *Neuroscience*, 34(16), 5603-5612.
865 Qi, F., Wu, A. D., & Schweighofer, N. (2011). Fast estimation of transcranial magnetic stimulation
866 motor threshold. *Brain stimulation*, 4(1), 50-57.
867 Rawji, V., Kaczmarczyk, I., Rocchi, L., Rothwell, J. C., & Sharma, N. (2019). Short interval intracortical
868 inhibition as measured by TMS-EEG. *BioRxiv*, 802504.
869 Reddan, M. C., & Wager, T. D. (2018). Modeling pain using fMRI: from regions to biomarkers.
870 *Neuroscience bulletin*, 34(1), 208-215.
871 Rocchi, L., Di Santo, A., Brown, K., Ibáñez, J., Casula, E., Rawji, V., . . . Rothwell, J. (2021).
872 Disentangling EEG responses to TMS due to cortical and peripheral activations. *Brain*
873 *stimulation*, 14(1), 4-18.
874 Rogasch, N. C., Sullivan, C., Thomson, R. H., Rose, N. S., Bailey, N. W., Fitzgerald, P. B., . . . Hernandez-
875 Pavon, J. C. (2017). Analysing concurrent transcranial magnetic stimulation and

876 electroencephalographic data: A review and introduction to the open-source TESA software.
877 *Neuroimage*, 147, 934-951.

878 Rohel, A., Bouffard, J., Patrício, P., Mavromatis, N., Billot, M., Roy, J.-S., . . . Masse-Alarie, H. (2021).
879 The effect of experimental pain on the excitability of the corticospinal tract in humans: A
880 systematic review and meta-analysis: *European Journal of Pain*, 25(6), 1209-1226..

881 Rossi, S., Hallett, M., Rossini, P. M., Pascual-Leone, A., & Group, S. o. T. C. (2009). Safety, ethical
882 considerations, and application guidelines for the use of transcranial magnetic stimulation in
883 clinical practice and research. *Clinical Neurophysiology*, 120(12), 2008-2039.

884 Rossini, P. M., Barker, A., Berardelli, A., Caramia, M., Caruso, G., Cracco, R., . . . Lücking, C. (1994).
885 Non-invasive electrical and magnetic stimulation of the brain, spinal cord and roots: basic
886 principles and procedures for routine clinical application. Report of an IFCN committee.
887 *Electroencephalography and clinical Neurophysiology*, 91(2), 79-92.

888 Rothwell, J. C., Hallett, M., Berardelli, A., Eisen, A., Rossini, P., & Paulus, W. (1999). Magnetic
889 stimulation: motor evoked potentials. The International Federation of Clinical
890 Neurophysiology. *Electroencephalography and clinical neurophysiology. Supplement*, 52, 97-
891 103.

892 Ruddy, K., Balsters, J., Mantini, D., Liu, Q., Kassraian-Fard, P., Enz, N., . . . Wenderoth, N. (2018).
893 Neural activity related to volitional regulation of cortical excitability. *Elife*, 7.

894 Salo, K. S.-T., Vaalto, S. M., Koponen, L. M., Nieminen, J. O., & Ilmoniemi, R. J. (2019). The effect of
895 experimental pain on short-interval intracortical inhibition with multi-locus transcranial
896 magnetic stimulation. *Experimental Brain Research*, 237(6), 1503-1510.

897 Schabrun, S. M., & Hodges, P. W. (2012). Muscle pain differentially modulates short interval
898 intracortical inhibition and intracortical facilitation in primary motor cortex. *Journal of Pain*,
899 13(2), 187-194. doi:10.1016/j.jpain.2011.10.013

900 Schneider, T., & Neumaier, A. (2001). Algorithm 808: ARfit—A Matlab package for the estimation of
901 parameters and eigenmodes of multivariate autoregressive models. *ACM Transactions on
902 Mathematical Software (TOMS)*, 27(1), 58-65.

903 Schulz, E., May, E. S., Postorino, M., Tiemann, L., Nickel, M. M., Witkovsky, V., . . . Ploner, M. (2015).
904 Prefrontal gamma oscillations encode tonic pain in humans. *Cerebral cortex*, 25(11), 4407-
905 4414.

906 Seminowicz, D. A., Thapa, T., Furman, A. J., Summers, S. J., Cavalieri, R., Fogarty, J. S., . . . Schabrun, S.
907 M. (2018). Slow peak alpha frequency and corticomotor depression linked to high pain
908 susceptibility in transition to sustained pain. *BioRxiv*, 278598.

909 Seminowicz, D. A., Thapa, T., & Schabrun, S. M. (2019). Corticomotor depression is associated with
910 higher pain severity in the transition to sustained pain: A longitudinal exploratory study of
911 individual differences. *The journal of Pain*, 20(12), 1498-1506.

912 Shirazi, S. Y., & Huang, H. J. (2019). More reliable EEG electrode digitizing methods can reduce
913 source estimation uncertainty, but current methods already accurately identify brodmann
914 areas. *Frontiers in neuroscience*, 13, 1159.

915 Silbert, B., Patterson, H., Pevcic, D., Windnagel, K., & Thickbroom, G. (2013). A comparison of
916 relative-frequency and threshold-hunting methods to determine stimulus intensity in
917 transcranial magnetic stimulation. *Clinical Neurophysiology*, 124(4), 708-712.

918 Summers, S. J., Chipchase, L. S., Hirata, R., Graven-Nielsen, T., Cavalieri, R., & Schabrun, S. M. (2019).
919 Motor adaptation varies between individuals in the transition to sustained pain. *Pain*,
920 160(9), 2115-2125.

921 Svensson, P., Cairns, B. E., Wang, K., & Arendt-Nielsen, L. (2003). Injection of nerve growth factor
922 into human masseter muscle evokes long-lasting mechanical allodynia and hyperalgesia.
923 *Pain*, 104(1-2), 241-247.

924 Tadel, F., Baillet, S., Mosher, J. C., Pantazis, D., & Leahy, R. M. (2011). Brainstorm: a user-friendly
925 application for MEG/EEG analysis. *Computational Intelligence and Neuroscience*, 2011.

926 Tremblay, S., Rogasch, N. C., Premoli, I., Blumberger, D. M., Casarotto, S., Chen, R., . . . Fitzgerald, P.
927 B. (2019). Clinical utility and prospective of TMS-EEG. *Clinical Neurophysiology*, 130(5), 802-
928 844.
929 van Doorn, J., van den Bergh, D., Böhm, U., Dablander, F., Derkx, K., Draws, T., . . . Haaf, J. M. (2021).
930 The JASP guidelines for conducting and reporting a Bayesian analysis. *Psychonomic Bulletin
931 & Review*, 28, 813-826.
932 Ye, Y., Wang, J., & Che, X. (2022). Concurrent TMS-EEG to reveal the neuroplastic changes in the
933 prefrontal and insular cortices in the analgesic effects of DLPFC-rTMS. *Cerebral Cortex*,
934 32(20), 4436-4446.
935

936

937

938

939

940

941

942

943

944

945

946

947

948

949

950

951

952

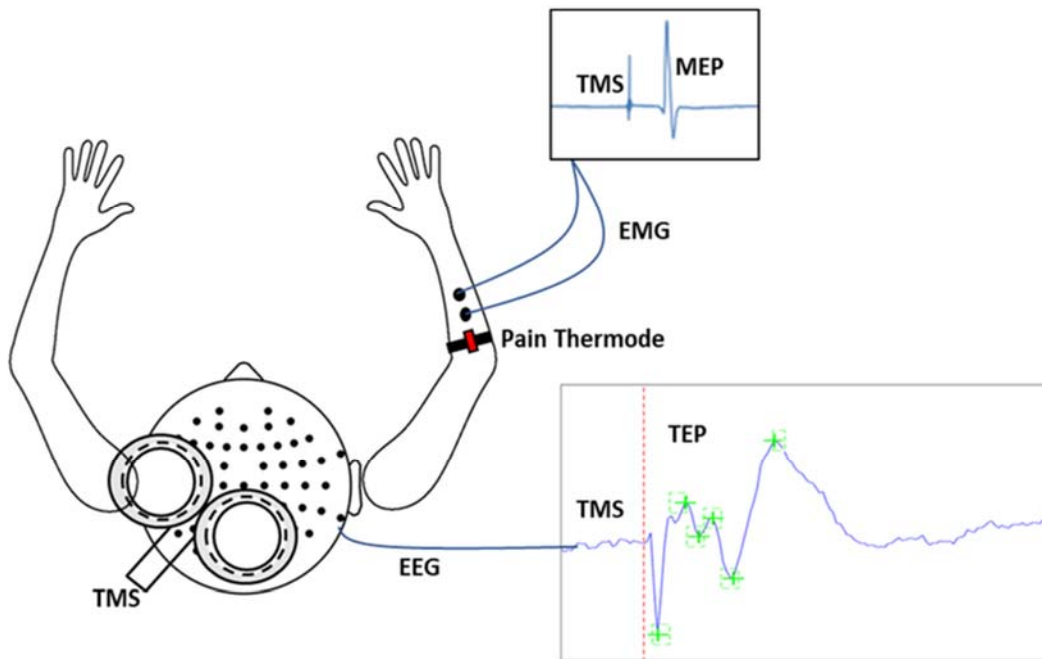
953

954

955

956

Figures



957

958

959 **Figure 1. Schematic of experimental apparatus.** This consisted of transcranial magnetic
960 stimulation (TMS) during concurrent electroencephalography (EEG) to simultaneously
961 record motor evoked potentials (MEPs) and TMS-evoked potentials (TEPs). MEPs were
962 recorded using electromyographic (EMG) electrodes placed over the distal region of the
963 extensor carpi radialis brevis (ECRB) while thermal pain was delivered over the proximal
964 region of the ECRB.

965

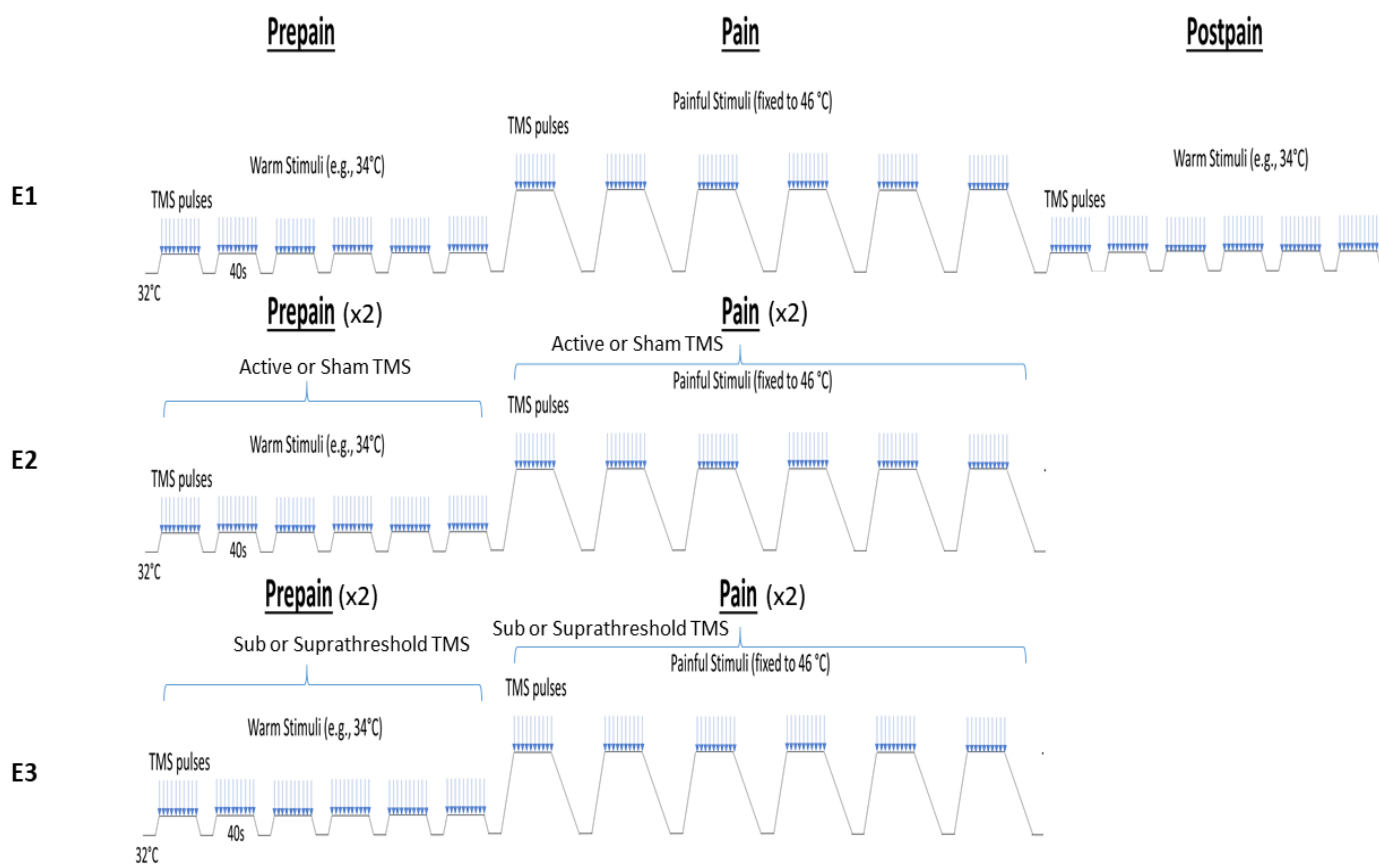
966

967

968

969

970



972 **Figure 2. Schematic of the experimental protocols.** In Experiment 1, participants
973 experienced three blocks of thermal stimuli: a pre-pain, pain, and post-pain block, with each
974 block consisting of multiple thermal stimuli delivered 40s at a time, and during which TMS
975 measurements (indicated by blue arrows) and verbal pain ratings were obtained. The pre-
976 pain and post-pain blocks involved thermal stimuli delivered at the warm threshold (i.e., the
977 temperature that leads to any perceived change in skin temperature from baseline). In the pain
978 block, thermal stimuli were delivered at 46°C. For Experiment 2, the post-pain block was
979 excluded, and an additional sham TMS condition was intermixed within both the pre-pain
980 and pain blocks. For Experiment 3, the post-pain block was also excluded, and an additional
981 subthreshold TMS condition intermixed within both the pre-pain and pain blocks.

982

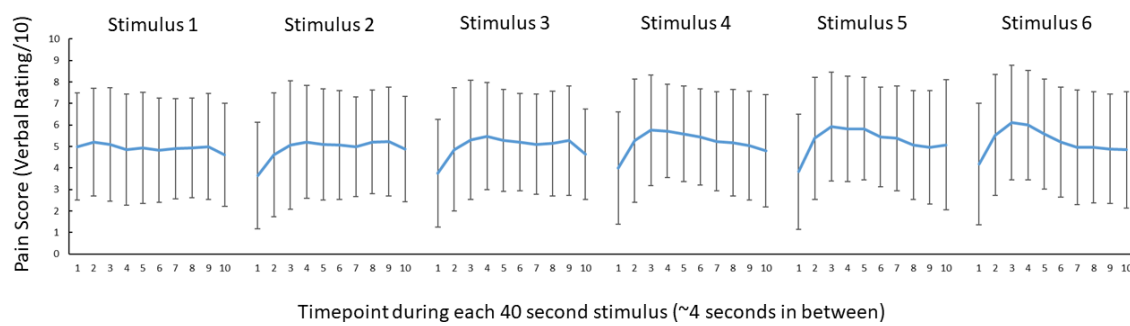
983

984

985

986

987



988

Timepoint during each 40 second stimulus (~4 seconds in between)

989

Figure 3. No conclusive evidence of a difference in pain ratings between successive 46°C 40s thermal stimuli. Mean (\pm SD) pain ratings during the 6 thermal stimuli delivered during the pain block (thermal stimuli delivered at 46°C) of Experiment 1. 10 pain ratings were collected over each 40 second thermal stimulus ~ every 4 second.

990

991

992

993

994

995

996

997

998

999

1000

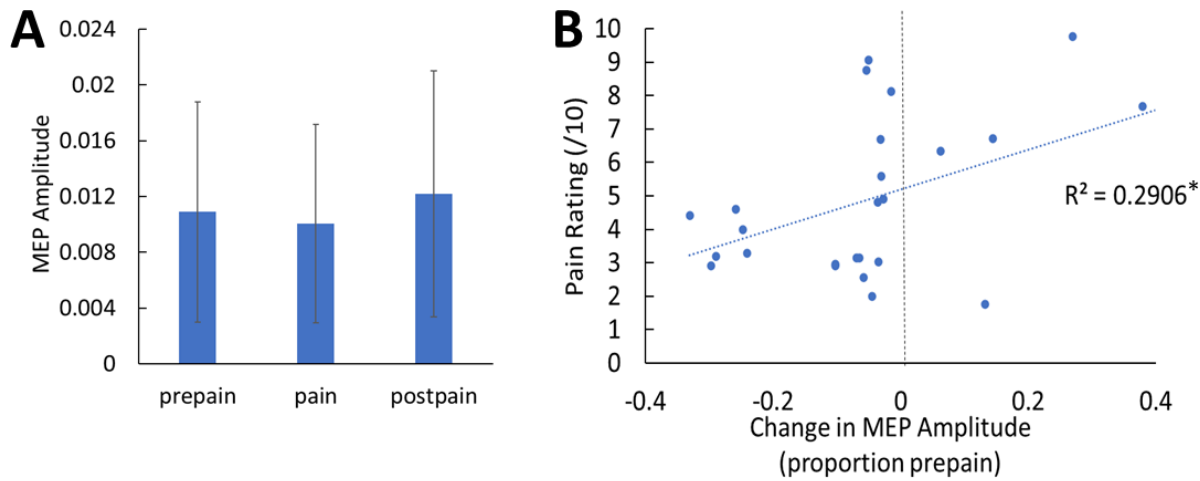
1001

1002

1003

1004

1005



1006

1007 **Figure 4. No conclusive evidence of MEP amplitude differences between conditions;**
1008 **however individual pain sensitivity was predicted by changes in MEP amplitude. A:**
1009 Mean (\pm SD) MEP amplitude during the pre-pain, pain and post-pain blocks of Experiment 1.
1010 B: Individual-level Relationship between change in MEP amplitude during pain (proportion
1011 of pre-pain) and mean verbal pain rating provided by each participant.

1012

1013

1014

1015

1016

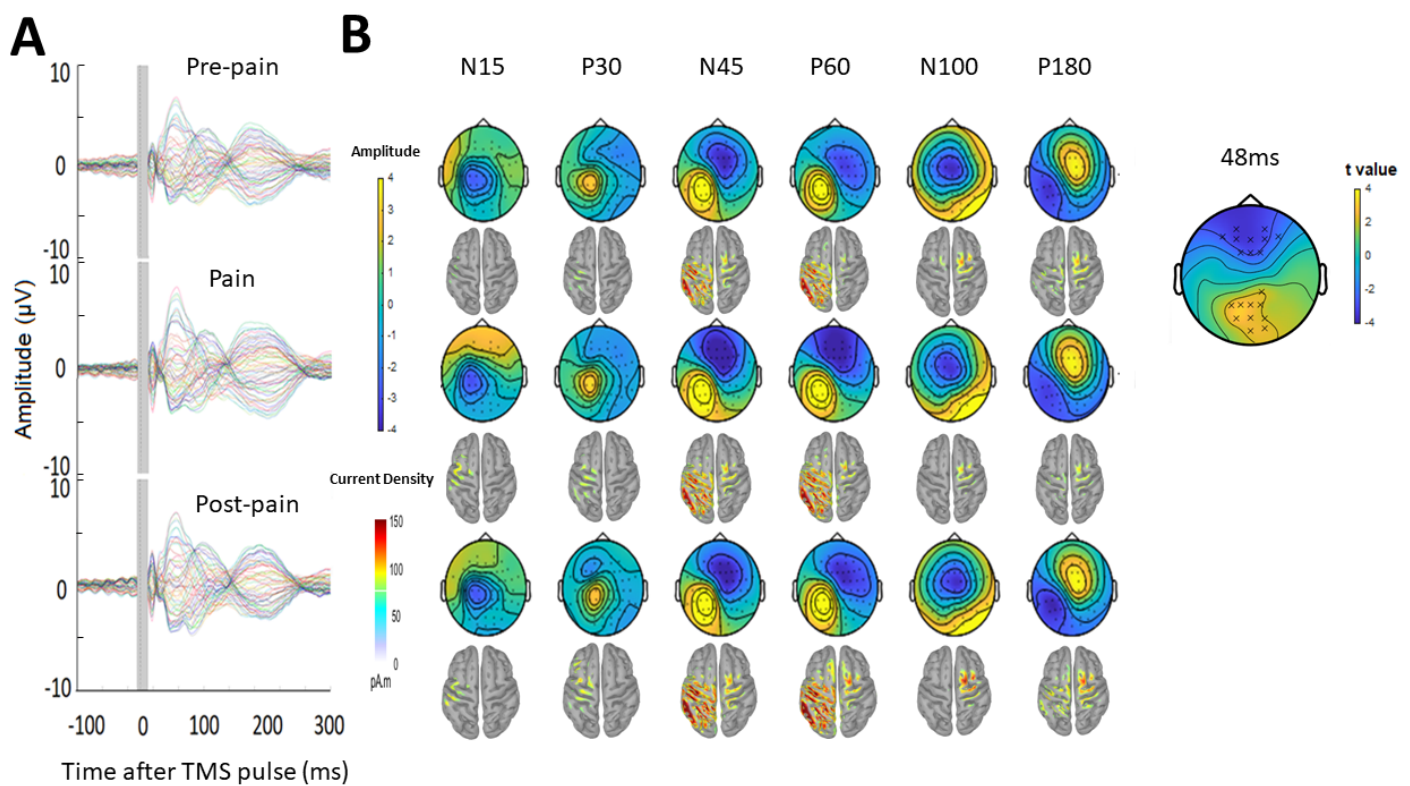
1017

1018

1019

1020

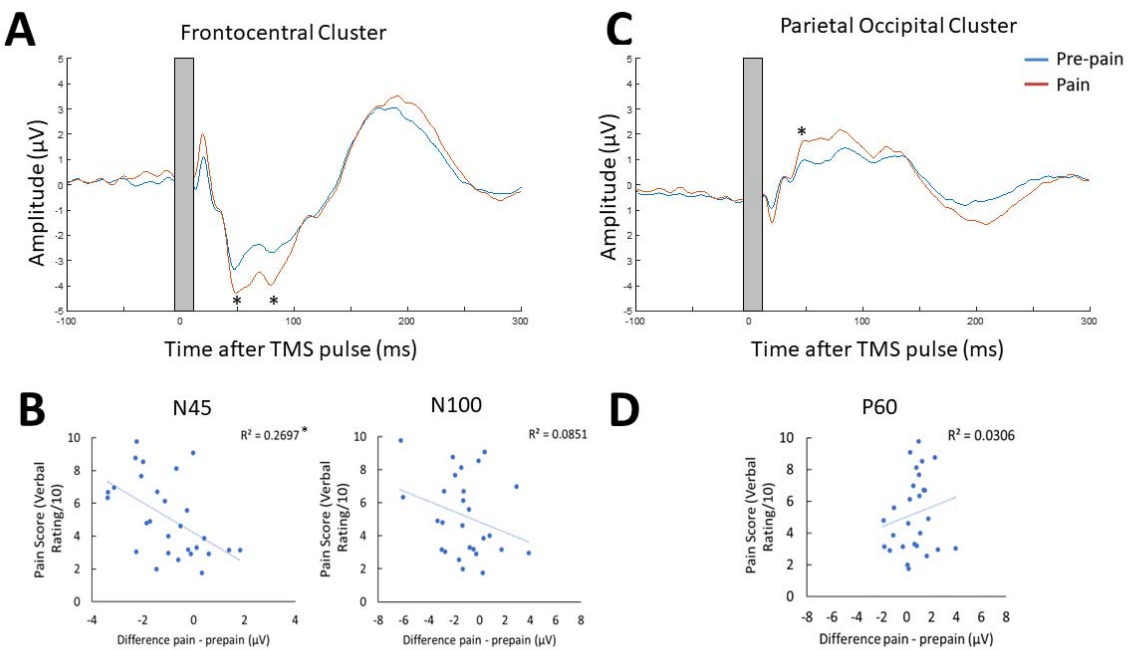
1021



1023 **Figure 5. Pain led to increased negative and positive amplitude in frontocentral and**
1024 **parietal-occipital sites respectively, 43-90ms after the TMS pulse. A:** Grand-average TEPs
1025 during the pre-pain, pain and post-pain blocks of Experiment 1. The grey shaded area
1026 represents the window of interpolation around the TMS pulse. **B:** Scalp topographies and
1027 estimated source activity at timepoints where TEP peaks are commonly observed, including
1028 the N15, P30, N45, P60, N100 and P180. A cluster plot is also shown on the right comparing
1029 signal amplitude between the pain and pre-pain conditions at a representative timepoint
1030 (48ms) between 43-90ms, which is where significant amplitude differences were observed.
1031 The black stars demonstrate the presence of significant positive (yellow) or negative (blue)
1032 clusters.

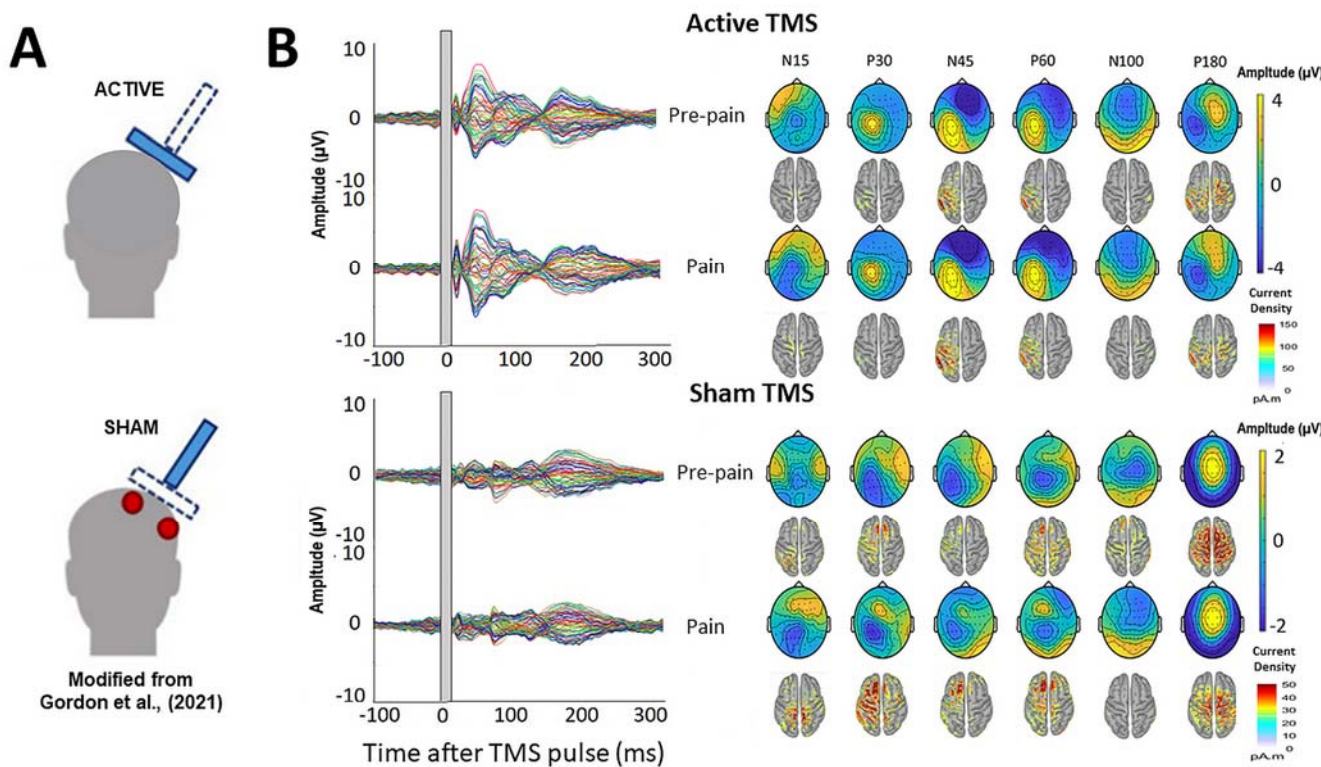
1033

1034



10:

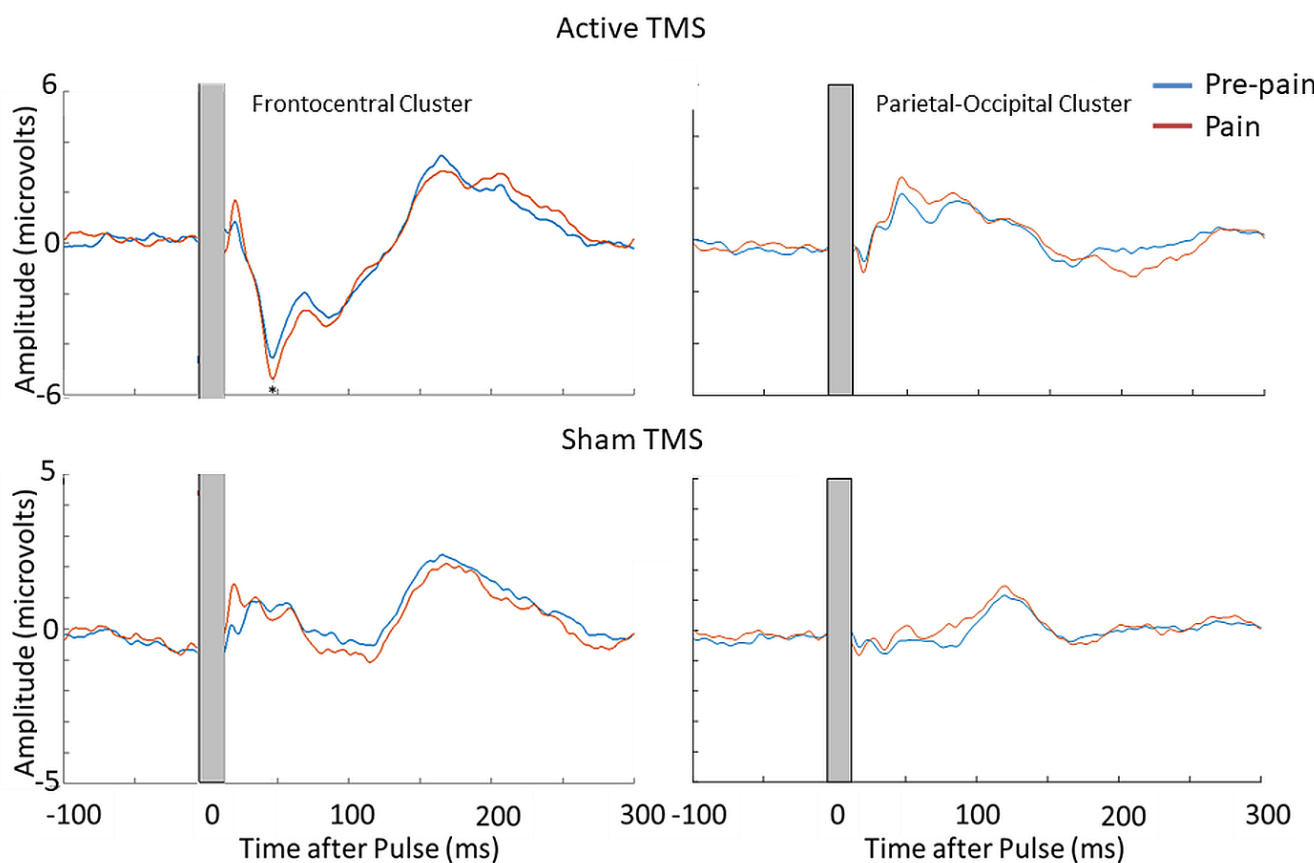
1036 **Figure 6. Pain led to increases in N45, P60 and N100 peak amplitude, and individual**
 1037 **pain sensitivity was predicted by changes in the N45 peak.** TEPs across pain and pre-pain
 1038 condition for the frontocentral electrodes (A) and parietal-occipital electrodes (C) identified
 1039 from the cluster analysis of Experiment 1. The grey shaded area represents the window of
 1040 interpolation around the transcranial magnetic stimulation (TMS) pulse. For the frontocentral
 1041 electrodes, two significantly stronger negative peaks were identified at ~45 and 85ms post-
 1042 TMS. For the parietal-occipital electrodes, a significantly stronger positive peak was
 1043 identified at ~50ms post-TMS. * indicates at least moderate evidence the alternative
 1044 hypothesis that the amplitude is larger in pain vs. pre-pain ($BF_{10} > 3$). Individual-level
 1045 relationship between mean verbal pain ratings provided by each participant and change in
 1046 peak amplitudes at ~45ms (N45), ~85ms (N100) post-TMS (B), and ~50ms (P60) post-TMS
 1047 (D).



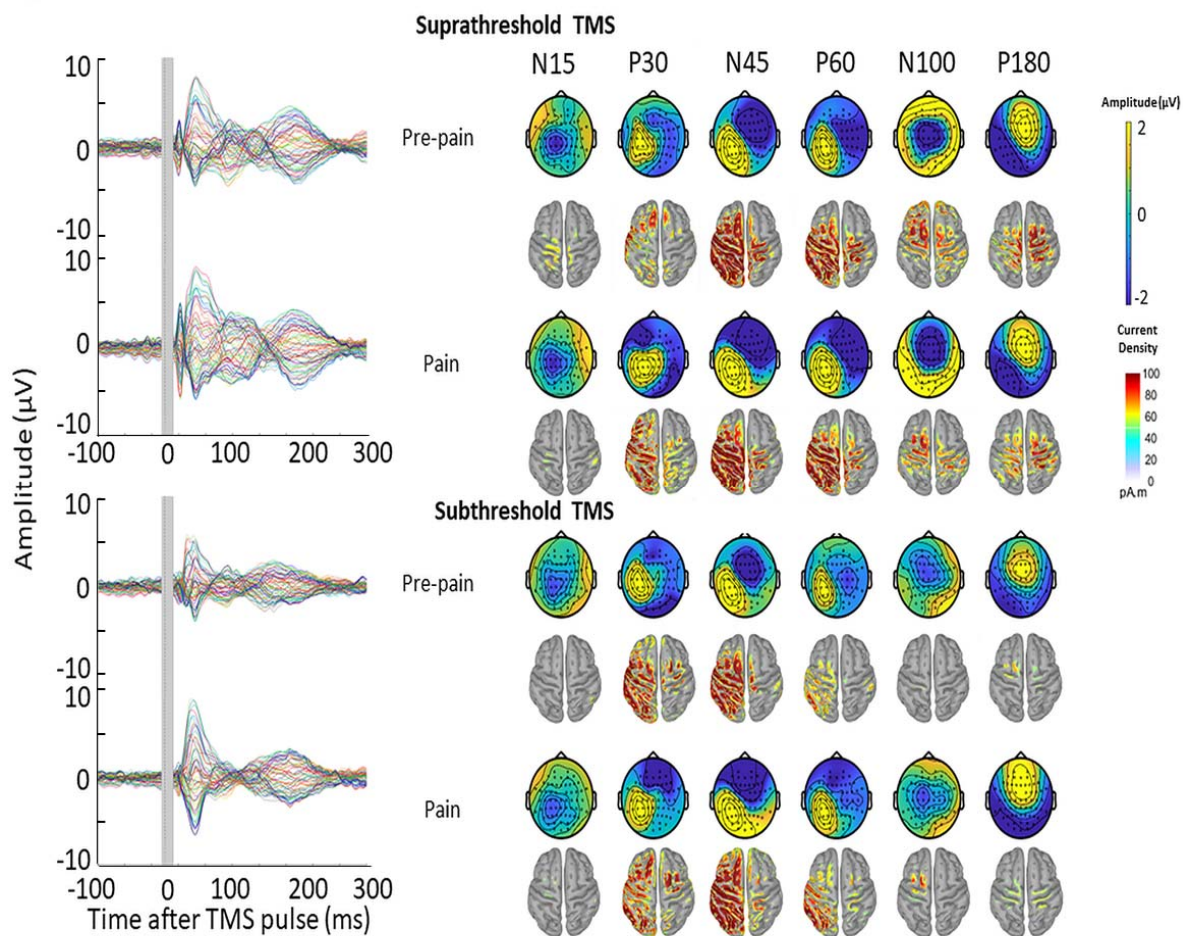
1049 **Figure 7. TMS-evoked potentials for Active and Sham TMS.** A: Schematics showing the
1050 delivery of active and sham TMS of Experiment 2. Sham TMS involved scalp electrical
1051 stimulation (in red) beneath a sham coil (in dotted blue) to mimic somatosensory stimulation
1052 associated with active TMS, and concurrent delivery of active TMS 90 degrees to the scalp
1053 (in shaded blue) to mimic auditory stimulation associated with TMS. B: Left: TEPs during
1054 the pre-pain and pain blocks, for both active and sham stimulation. The grey shaded area
1055 represents the window of interpolation around the TMS pulse. Right: Scalp topographies and
1056 estimated source activity at timepoints where TEP peaks are commonly observed, including
1057 the N15, P30, N45, P60, N100 and P180.

1058

1059



1061 **Figure 8. Pain led to an increase in the N45 peak amplitude during active TMS but not**
1062 **sham TMS.** TEPs during pain and pre-pain blocks, across active and sham TMS conditions
1063 of Experiment 2, for the frontocentral electrodes (left) and parietal occipital electrodes (right)
1064 identified from the cluster analysis in the main experiment. A significantly stronger
1065 frontocentral negative peak was identified ~45ms post-TMS during pain compared to pre-
1066 pain, for the active TMS condition. * indicates at least moderate evidence the alternative
1067 hypothesis that the amplitude is larger in pain vs. pre-pain ($BF_{10} > 3$). The dotted line shows
1068 the timing of the peak.
1069

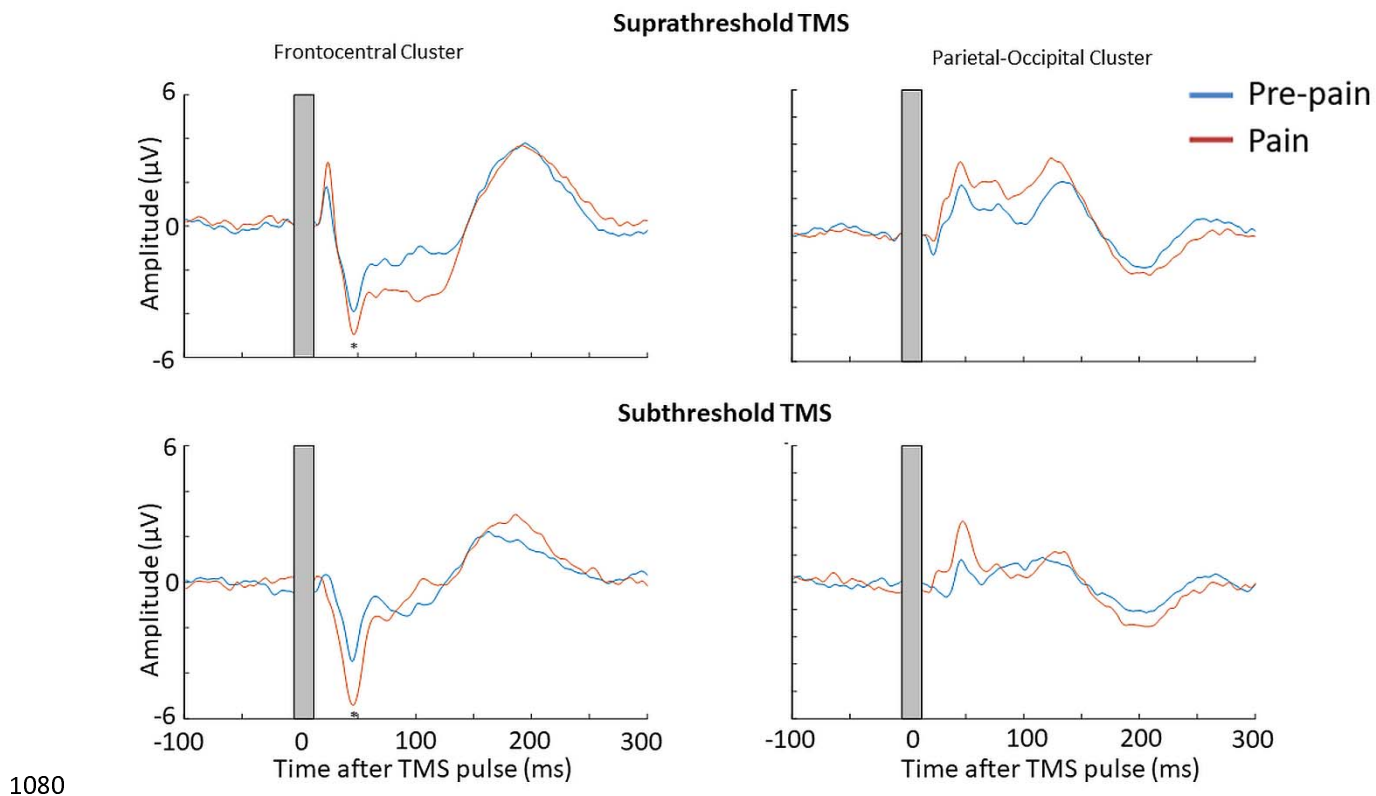


1070

1071

1072 **Figure 9. TMS-evoked potentials for supra- and subthreshold TMS.** Left: TEPs during
1073 the pre-pain and pain blocks, for both supra- and subthreshold TMS of Experiment 3. The
1074 grey shaded area represents the window of interpolation around the transcranial magnetic
1075 stimulation TMS pulse. Right: Scalp topographies and estimated source activity at timepoints
1076 where TEP peaks are commonly observed, including the N15, P30, N45, P60, N100 and
1077 P180.
1078

1079



1080
1081 **Figure 10. Pain led to an increase in the N45 peak amplitude for both suprathreshold**
1082 **and subthreshold TMS.** TEPs during pain and pre-pain blocks of Experiment 3, across
1083 supra- and subthreshold TMS conditions, for the frontocentral electrodes (left) and parietal
1084 occipital electrodes (right) identified from the cluster analysis in Experiment 1. A
1085 significantly stronger frontocentral negative peak was identified ~45ms post-TMS during
1086 pain compared to pre-pain for both supra- and subthreshold stimulation. * indicates at least
1087 moderate evidence the alternative hypothesis that the amplitude is larger in pain vs. pre-pain
1088 ($BF_{10} > 3$). The dotted line shows the timing of the peak.
1089

1090

1091

1092

1093

1094

1095

1096

1097